A COMPREHENSIVE REVIEW
Pool Boiling Using Nanofluids

by

Asif KHAN[a] and Hafiz Muhammad ALI[b,*]

[a]Mechanical Engineering Department, University of Engineering and Technology, Taxila, Pakistan
[b]Mechanical Engineering Department, King Fahd University of Petroleum and Minerals, Dhahran, Saudi Arabia

Review paper
https://doi.org/10.2298/TSCI190110072K

Nanofluids are suspensions of nanoparticles with small concentration spread in base fluids such as water, oil and ethylene glycol. Nanofluid boiling is an important research area which provides many chances to explore new frontiers but also poses great challenges. Over the last decade, various studies have been carried out on pool boiling of nanofluids for the enhancement of critical heat flux which is otherwise limited by the use of base fluids. Several efforts have been made in the literature on nanofluid boiling, however, data on the boiling heat transfer coefficient and the critical heat flux have been unpredictable. Current study is a review of the status of research work on effects of nanofluids on heat transfer coefficient and critical heat flux. An emphasis is put in a review form on the recent progresses in nanofluid heat transfer coefficient and critical heat flux of pool boiling. This study also focuses on advancements in nanofluids, their properties and various parameters affecting boiling critical heat flux and heat transfer coefficient. At the end correlations used by different researchers to find out the critical heat flux and heat transfer coefficient are listed.

Keywords: *nanofluids,* critical heat flux*, heat transfer coefficient, boiling, enhancement*

Introduction

Boiling heat transfer is usually employed in many areas of science and technologies because it is an effective way to dissipate heat. Boiling heat transfer is used with great interest to cool electronics chips and nuclear reactors, computers, nuclear and fossil energy systems. Critical heat flux (CHF) restricts the boiling heat transfer efficiency. For the development of novel approaches numerous studies have been conducted so far to increase CHF values. Another great important concern in heat transfer is increasing heat transfer coefficient (HTC). For the effectiveness of heat transfer and factors which are involves to increase HTC, different studies are carried out and therefore new techniques have been developed. Pool boiling performance can greatly be affected by wettability changes and topography of the surface [1, 2]. Pool boiling plays an important role in high performance thermal management. Nanofluids are used to enhance heat transfer. Nanofluids are prepared by dispersion of nanosize particles in base fluids [3]. Based on single phase heat transfer in several systems, enhanced thermal conductivity has

* Corresponding author, email: hafiz.ali@kfupm.edu.sa

been demonstrated in these suspensions as compared to base fluid. To investigate nanofluids in phase change heat transfer for potential enhancement, extensive research has also been performed. Thermal management systems such as microelectronics [4, 5], HVAC systems [6], automotive industry [7, 8], solar collectors [9, 10], cooling system in electronics [11, 12], and nuclear reactors [13, 14] use nanofluids to improve heat transfer and thermal efficiency. These are used in light water reactors due to their capability to manage strategy in severe accidental conditions to enhance the in-vessel retention capability [15]. In order to reduce cost and to provide significant energy, nanofluids with high thermal conductivity can be used [6].Use of nanofluids makes the thermal system smaller and light in weight. There is a linear relation between Fe particle up to 0.55 vol.% and thermal conductivity up to 18% [16].

Nanofluids can increase, decrease or in some cases have no effect on pool boiling heat transfer was the pioneer study of [17]. To explain the same phenomena a review was presented by [18] and now several theories are available. There is always an enhancement in CHF with nanofluids in contrast to these varying trends for nucleate pool boiling [19]. Enhancement percentage depends on the size, shape and concentration of particles, as well as, on the consistency of the nanofluid and the presence of additives [20, 21]. Nanoparticles are added to the base fluid to enhance the pool boiling heat transfer when performance of the base fluid is not up to the mark due to limitations of its thermal properties. Rather, microlayer evaporation phenomenon that creates modifications of microlayer has greater influence [22, 23]. Surface wettability increases when the nanoparticle present in liquid deposits on the surface during vaporization of the liquid present in the microlayer. When the microlayer evaporates containing liquid having nanoparticle, it adversely affects the heat transfer performance [23-25]. There is no difference either we use nanofluids to enhance heat transfer or nanofluids coated surface [26]. In contrast to the above works, highly stable nanofluids were used by [27] and surface functionalized nanofluids were developed earlier by [28]. These novel nanofluids have minimal surface deposition on the boiling surface. Thermal performance enhancement is highly affected by thermophysical properties of those nanofluids which do not affect boiling surface. These specially designed functionalized nanofluids are only solution over conventional nanofluids.

Present work is a review of effect of nanofluids on CHF, HTC in pool boiling heat transfer and reasons behind their increment/decrement. It also reviews the characteristics of thermophysical properties of nanofluids during pool boiling. Different correlations developed by researchers in pool boiling heat transfer and CHF are also listed down at the end of this work.

Experimental studies on pool boiling using nanofluids

Some of the experimental effects on CHF and HTC in pool boiling using nanofluids are briefly reviewed in this section.

Experimental studies on CHF

This section is divided into three sub-section based on the heat providing method to boil nanofluid.

Boiling of nanofluid through heating tube/rod:

In this type of experimental setups, to boil nanofluid, a heating module mostly located at the bottom of the test chamber consists of power input electrodes, a resistive wire heater for the steady state heat transfer. A simple wire heater pool boiling setup used by [29] is shown in fig 1.

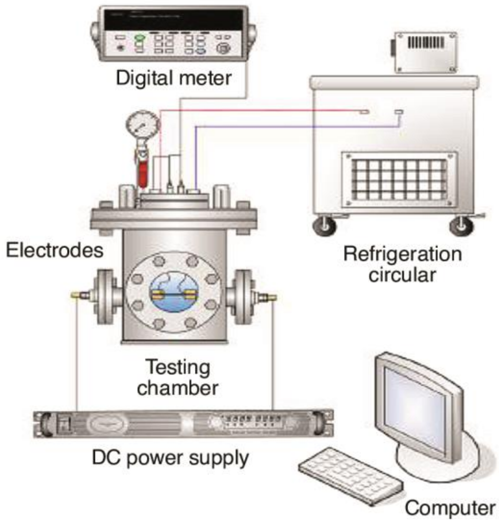

Figure 1. Experimental set-up used by [29]

Pool boiling CHF was enhanced with Al_2O_3-water nanofluid. Authors used three different powder sizes of Al_2O_3 which were 0.05, 0.3, and 1.0 μm. Addition of alumina particle in water increases the boiling heat flux [30].

Experiments were conducted using three different concentrations (0.25, 0.5, and 1%) of copper nanoparticle in water with 9.0 wt.% of sodium dodecyl sulfate (SDS) as a surfactant. It is concluded that increasing the concentration of nanoparticle in base water decreases the pool boiling coefficient of heat transfer. The CHF increases by 50% and 60% with the increase of concentration of nanoparticles in water and adding surfactant in water, respectively, [31].

The CHF was significantly enhanced using titania and alumina nanoparticles in water as compared to pure water. Average size of nanoparticle used was 85 nm measured by scattering electron microscope. Enhancement in CHF is due to nanoparticle coating on heating surface [32].

Characteristics of nucleate boiling are greatly affected by the operating pressure. miniature flat heat pipe with evaporator having micro grooved heat transfer surface gives 50% increment in CHF at atmospheric pressure whereas this value increases up to 150% at 7.4 kPa pressure [33]. Experiments were conducted with three water based nanofluids named diamond, zinc oxide and alumina on passively engineered heat transfer surface. Test section was made of stainless steel. Average size of nanoparticle was measured using dynamic light scattering (DLC) which was 1.91 μm. It was concluded that pool boiling CHF increased up to 35% with pre-coated heaters [34].

Water based functional nanofluids have nearly no effect on CHF. Experiments were conducted with silica/water nanofluids. Scattering electron microscope was used for measurement of nanoparticle size. It was concluded that due to change of thermal properties of nanofluids, there is no significant effect on CHF [35]. Experiments were conducted with suspended silica nanoparticle using nicrome wire and ribbons to investigate both CHF and burnout heat flux (BHF). Influence of heater surface dimension, cross section shape as well as surface modification was checked. The CHF and BUF decreases with the increase in heater surface area. High heat transfer occurs due to deposition of particle at a concentration of (0.1-0.2 vol.%). It was concluded that for ribbon type heater there is maximum of 270% CHF enhancement [36]. The Fe_3O_4/ethylene glycol-water nanofluid were tested using thin Ni-Cr wire at atmosphere pressure with and without electric field. The size of nanoparticle used was 100 nm. It was concluded that 1 vol.% of nanofluid enhances CHF to 100%. Surface wettability plays vital role in CHF enhancement [37].

Copper plate was used to examine the CHF enhancement using Al_2O_3-water nanofluid. Concentration of Al_2O_3-water used in this study was 0-0.1 vol.%. The size of nanoparticle used was 45 nm measured by DLC. A polyvinyl alcohol was used as a stabilizer. It was concluded that effective boiling surface area is responsible for increase in CHF [38]. Magnetite-water nanofluid on Ni-Cr wire was used to investigate the CHF performance. As nanoparticle concentration increases, CHF also increases. This enhancement was approximately 170% to 240% as compared to pure water [39]. The Al_2O_3 based aqueous nanofluid was used on flat plate test section. Average size of nanoparticle was 40 nm given by atomic force microscope. It was concluded that for 0.1 vol.% concentrations of nanofluid, CHF increases. They reported that CHF enhancement is due to volume fraction of nanoparticle [40]. Experimental investigation was carried out on saturated pool boiling CHF with Ni-Cr nanoparticle having coating thickness of 50 nm at atmosphere pressure at 0.01 vol.% alumina. Long pre coating time decreases CHF [41].

Experimental investigation was carried out for transient pool boiling characteristics using graphide oxide nanosheets (GON) on copper sphere. Sizes of nanoparticle used were 200-500 nm measured by transmission electron microscope. The dilute concentrations of GON used were <0.001 wt.%. Increasing the GON concentrations CHF increases [42]. Boiling characteristics were examined with ZnO, SiO_2, SiC, Al_2O_3, graphene oxide (GO), and CuO nanoparticles at 0.01% volume concentration on 0.49 mm diameter cylindrical Ni-Cr wire heating element. Distilled water and R-123 were used as base fluids. It was observed that compared to distilled water all nanofluids enhance heat transfer in the range 90-160% [43]. The CHF performance was examined with Al_2O_3 and magnetite (Fe_3O_4) nanoparticle in water using Ni-Cr wire. Average sizes of nanoparticles were 25 nm and 20-30 nm for magnetite and alumina, respectively. Test pressure ranged from 101 Kpa to 1100 Kpa. Authors concluded that CHF increases with nanoparticle concentration at higher pressure [44]. Reduced graphene oxide (RGO) colloid was used with 0.0005 wt.% flake-based RGO in distilled water. The Ni–Cr thin-wire heaters were used for heating purpose. To study the coating time of RGO flake aggregation, coatings at both the sides were tested along with single sided. Cathode side of the wire which has thin well-aligned RGO layer coating CHF enhanced by 20% whereas uniform RGO coating layer caused increase in CHF upto 320% [45].

Using various ionic concentrations of silica nanofluids in pool boiling, different acidity and base solutions were analysed. The CHF increases three times with silica suspension as compared to conventional fluids. Presence of salts decreases the catalytic property of nanofluids and there is a thicker double diffuse layer with 10 nm particles as compared to 20 nm particles. Authors reported that nanofluids in buffer solutions allow a lesser CHF than in strong electrolyte *i. e.* in high ionic concentration [46]. To investigate the CHF enhancement experiments were performed using different concentrations of GO nanoparticles in base fluid. Nichrome wire with 0.2 mm diameter was used as a heating source. It is found that GO flakes formed a smooth laminated film which increases the CHF [47]. An experimental study was carried out with γ-Fe_2O_3 nanoparticle on a 100 μm platinum wire at 1 bar pressure. Average size of nanoparticle was 10 nm given by scattering electron microscope. Deposition of charged surface coating was obtained and boiling CHF increases [48].

Effect of ammonia and graphene/graphene-oxide nanosheets with variation in wavelength was investigated. Nanoparticles size used were >45 nm given by scattering electron microscope. Heat transfer increases with nanofluids. They used the famous eq. (1), to find the effect of wavelength on critical heat transfer [49]:

$$q''_{\text{porous}} = \frac{\pi}{8} h_{fg} \left(\frac{\sigma \rho_g}{\lambda_m} \right)^{1/2} \tag{1}$$

Small cylinders ranging (11-510 μm) with three test liquids FC-72, R-113 and methanol were experimented. Size of nickel wire used for FC-72 was 11 μm. It was found that for dimensionless radius (R') values as low as 0.0123 hydrodynamic CHF mechanism was observed [50]. This experimental result modified the Sun and Lienhard CHF correlation equation for ($R' < 0.0123$) which is given as:

$$\frac{q_{\max}}{q_{\max_2}} = 0.89 + 1.01\mathrm{e}^{-2.18\sqrt{R'}}, \quad R' > 0.0123 \tag{2}$$

It was pointed out that change in wavelength enhanced the CHF.

It has been observed for all nanofluids that as temperature increases above the saturation point, boiling starts. As temperature increases pool boiling heat flux increases. Maximum heat flux is different for each nanofluid but maximum heat flux is usually observed between 20 °C to 40 °C. Among all nanofluids studied in this section, it is observed that TiO_2 nanoparticle coating on Ni-Cr wire gives maximum heat flux value which is approximately 2600 KW/m^2 as shown in fig 2.

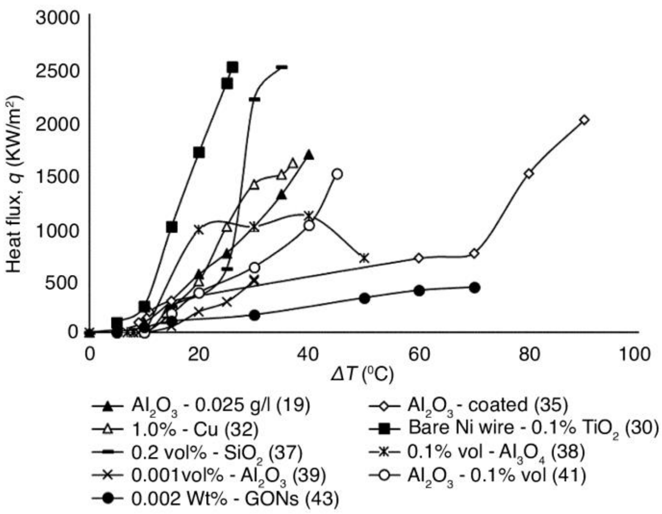

Figure 2: Comparison of boiling curves for different nanofluids

Boiling of nanofluid through square plate heater

In this method heat is provided to nanofluid through a plate heater through conduction. Mostly copper electrodes are used as a heat resistivity source to heat the plate. Like rod heater heat of fluids are measured by thermocouple inserted into fluids. A sample of experimental set-up using square/rectangular plate for heating used by [51] is shown in fig 3.

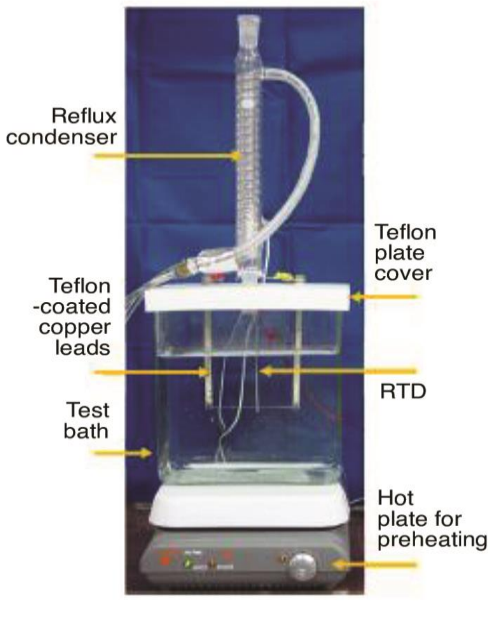

Figure 3. Experimental set-up used by [51]

Experiments were performed with water and water based zinc oxide nanofluid on stainless steel plate heaters. Zinc oxide nanoparticle with water as base fluid enhanced CHF for steady state pool boiling as compared to water. On the other hand for deionized water, transient CHF is higher than steady state CHF [52]. Experiments were conducted on 10 mm diameter upward facing plain copper heater at atmosphere pressure with saturated Al_2O_3-water nanofluids. The SEM ensures the nanoparticle coating layer on test section. The CHF was 2096 KW/m^2 with nanofluids boiling compared to water boiling which was 1532 KW/m^2. Nanoparticle coating layer is the reason behind enhancement in CHF [53].

Experiment was conducted with copper nanoparticle and sodium lauryl sulphate anionic surfactant (SDS) with 9 wt.% on stainless steel section. Atomic force microscopy characterised the averaged size of nanoparticle as 10 nm. When the concentration of copper nanoparticle in the base fluid increases CHF also increases. On the other hand there was 48% enhancement in CHF with nanofluids without using surfactant [54]. Experiment was conducted on brass rod for the quenching ability of SiO_2-water nanofluids. Average size of SiO_2 was 45 nm given by X-ray diffusion. As surface wettability increases CHF increases but HTC decreases [55]. Quenching behaviour of nanofluids on brass rod was analysed with different volume fraction of nanofluids (Al_2O_3, SiO_2, TiO_2, and CuO). Porous layer changes the surface roughness [56]. The TiO_2 coated surface formed on 12 nm horizontal heater surface enhanced CHF 1.7-1.8 times as compared to uncoated surface at atmosphere pressure [57]. An experimental investigation was carried out with FC-87 as nanofluids on enhanced copper surface with porous fin tops on open micro channels. Authors achievement in maximum CHF enhances to 37 W/cm^2 which if compared to a plain chip translates to 270% [58]. Heat flux versus temperature difference graph of previous researches studied in this section is shown in fig. 4.

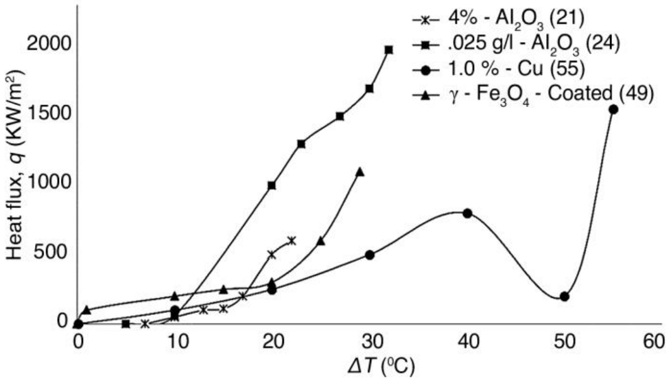

Figure 4. Comparison of boiling curves given by different researchers

It has been observed for all nanofluids that as temperature increases above the saturation point, boiling starts. As temperature increases heat flux increases. This trend is usually observed between 20 °C to 60 °C. Using rod as heating source alumina gives its maximum heat flux which is 2000 KW/m^2 at 32 °C. After this point heat flux starts decreasing.

Boiling of nanofluid through circular plate

The set-up most commonly used by the previous researchers for pool boiling consists of a heating device which is usually mounted concentrically at the bottom of the heating block. The vessel is completely insulated and heat is transferred through one direction conduction from plate. Thermocouples are embedded at top end of block to measure the amount of heat transfer though block to nanofluids. A cover plate at top end

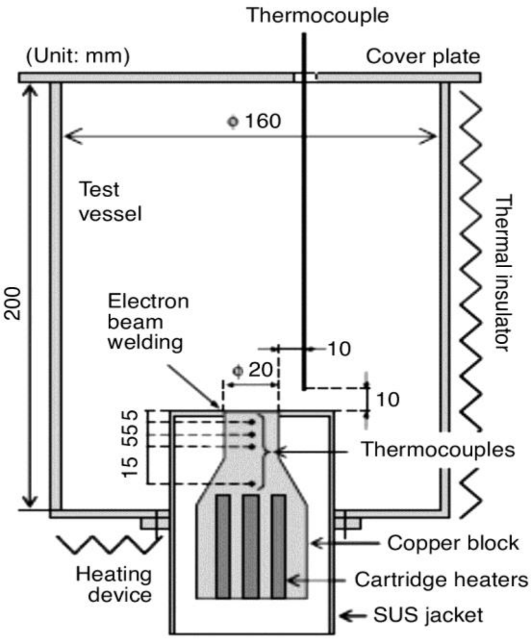

Figure 5. Schematic diagram of experimental apparatus used by [59]

of vessel is usually mounted to measure the fluid temperature. A sample of circular plate heat transfer assembly used by [59] is shown in fig. 5.

Nucleate boiling characteristics using CuO and SiO_2-water nanofluids were investigated. When the wall temperature crossed 112 C$^{\circ}$ agglutination phenomena occurred. Porous agglutination layer forms due to instability. No agglutination phenomena occurred using nanofluids. Nanoparticle sorption layer increases CHF. This layer is formed when there is a decrement in solid-liquid contact angle [60]. Addition of carbon nanotube (CNT) to base liquid increases the CHF. Transmission electron microscope confirms the average size of nanoparticle as 15 nm. Authors found that by decreasing pressure below atmospheric condition, CHF increases to 200% with CNT-water nanofluid as compared to deionized water [61]. The SiC-water nanofluid having 100 nm size with three volume concentrations 0.001%, 0.001%, and 0.01% were tested. The size of nanoparticle was confirmed by scattering electron microscope. Authors concluded that at 0.01% of nanoparticle, CHF enhanced to 105% [62]. Deposition of ZnO nanoparticle on heating surface increases the CHF. The ZnO-water nanofluid experimentation resulted that CHF was at least 54% higher with ZnO nanofluid as compared to deionized water due to nanoparticle layer formed on heater surface [63]. Presence of honeycomb porous plate with TiO_2-water increases the CHF. Size of nanoparticle used was 21 nm. There were 3.1 MW/m^2, 2.3 MW/m^2, and 2.2 MW/m^2 enhancements in CHF at 10 mm, 30 mm, and 50 mm diameter surfaces respectively [64].

Alumina and silver nanoparticle used in deionized water with circular plate heater at atmospheric pressure. Boiling curves shifted towards right for all nanofluids which shows enhancement in CHF. On the other hand, in the case of silver nanofluids, CHF enhanced more in small dispersion of nano *i. e.* at 0.01 g/l fluids as compared to large dispersion but after these point CHF decreases [65]. Nitric acid introduces the higher electrostatic force in TiO_2-water nanofluids. It was reported that without using nitric acid CHF of nanofluids increases up to concentration of 10^{-4} vol.% and remains constant thereafter. Copper block was used as a heating surface. Transmission electron microscope ensured the size of nanoparticle as 85.3 nm [66]. Stainless steel tube was used at different orientation angle ranging from 0° to 90° with three different nanofluids. These nanofluids were 0.05% Al_2O_3, 0.05% CNT +10% boric acid and 0.05% Al_2O_3. It was found that all these nanofluids enhanced CHF significantly (up to 220%) as compared to deionized water. Increasing the orientation angle increases CHF [67]. Figure 6 shows the enhancement in heat flux with temperature difference.

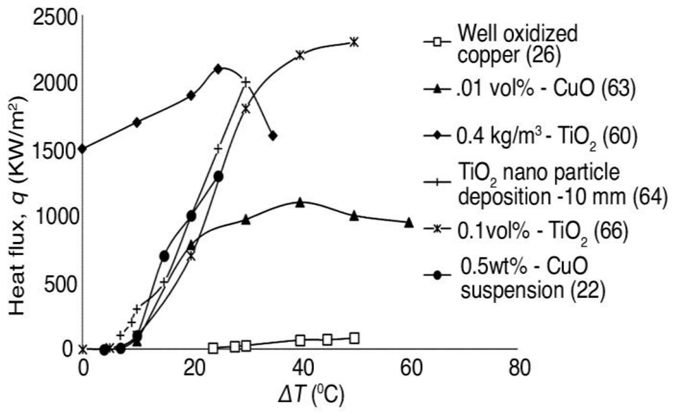

Figure 6. Boiling curves for different nanofluids

It has been observed for all nanofluids that as temperature increases above the saturation point, boiling starts. As temperature increases heat flux increases. This trend is usually observed between 20 $^{\circ}$C to 55 $^{\circ}$C. Using circular plate as heating source TiO_2-water nanofluid gives maximum value of heat flux which is 2400 KW/m^2 at 48 $^{\circ}$C.

Effect on CHF using nanofluids has been discussed in this portion. According to [19, 21, 31, 33. 40, 43, 45, 49, 52, 53, 55, 61, 62, 64] CHF increases by adding nanoparticle in base fluid as compared to water. In [23, 32, 67] concluded that due to contact angle formed between bubble and surface of heater, CHF increases. At higher temperature this angle changes from 90 °C to lower value. Heat flux increases by adding fins and microgroove heat transfer surface [34, 69]. In [22, 33, 46, 48, 54, 58, 63] concluded that main reason in the enhancement of heat flux is due to the formation of surface coating of nanoparticle on heating surface. According to [24, 26, 30, 36, 38, 49, 56] surface wettability increases the CHF. In [37, 39, 41] concluded that as effective surface area of heating increases CHF increases. Reference [47] reported that nanofluids in buffer solutions allow a lesser enhancement in CHF than in strong electrolyte *i. e.* in high ionic concentration. According to [50, 51] variation in wavelength property of certain nanofluids due to porous surface structure enhance CHF. According to [57] surface roughness is formed on heating surface due to deposition of nanoparticles. This roughness increases CHF. More rough surface causes more CHF.

Reasons for increase/decrease in CHF

Thermophysical properties attribution changes the boiling heat transfer with surface properties variation during nanofluid boiling. There is a significant CHF enhancement with nanofluids having low nanoparticle concentration but these nanofluids have less effect on thermophysical properties [31]. At low concentrations, changes in thermophysical properties of nanofluids are not responsible for CHF enhancement (<0.01 vol.%). This hypothesis were explained by [32] in which they used heating wire with clean surface and nanoparticle coating surface in which they observed the same CHF enhancement with both the wires. The CHF enhancement is directly proportional to surface roughness. Rough and wavy surfaces result higher surface superheat [21]. Deposition of nanoparticles becomes more by splitting of existing surface cavities into more cavities which increase CHF [24]. Added number of nanoparticle and layer built on heating surface also has a critical role in CHF [57]. Nanoparticle layer increases the liquid trapping to surface and thus vapour layer remains far away from liquid surface which delays nucleate boiling incipience [67]. The CHF does not increase when nanoparticle concentration thickens beyond a certain limit [31]. Active nucleation sites decrease with nanoparticle layers which significantly increases surface wettability (or less contact angle). As contact angle increases CHF decreases as there exist an inverse relationship [25]. In short surface wettability increases with increases in adhesion or surface roughness. It is seen that to increase CHF surface wettability should be enhanced which prevents vapour film [21]. Capillary plays an important role in CHF enhancement when the contact angle approaches zero during pool boiling experiment. In this way dry region under the vapour bubbles becomes wet due to capillary effect which delays CHF [24]. The effect on CHF of nanofluid is briefly given in tab. 1.

Table 1. Effect on CHF with parameter variation

Parameter Variation	CHF	Reason
Increase in surface wettability	Increase	Vapour formation is prevented so the number of active nucleation site decreases
Increase in capillarity	Increase	Dry region becomes wetted
Increase in surface roughness	Increase	Effective contact area increase, higher surface superheat

Table 2. gives the pool boiling effects summary with their effects on the enhancement of CHF.

Table 2. Summary of the pool boiling experiments and their effect on CHF

Ref.	Year	Heating surface	Particle size	Nanofluid	Surface analysis	ΔT [°C]	CHF enhancement [%]
[30]	1984	Stainless steel	0.05-1 μm	Al_2O_3-water	NA	28	Enhanced
[19]	2003	Cu block	< 10 nm	Al_2O_3-water	NA	40	200
[20]	2004	Ni-Cr wire	15 and 50 nm	SiO_2-water	NA	50	Enhanced
[21]	2005	NA	10 nm-100 nm	Al_2O_3-water	TEM	20	Enhanced
[25]	2010	Cu block	45nm	Al_2O_3-water	NA	45	37
[22]	2009	Ni-Cr wire	46 nm, 38 nm	Al_2O_3-water BiO_2-water	JEM-3010, Nanophase Technologies	NA	50 (Al_2O_3-water) 33 (BiO_2-water)
[31]	2009	Seamless Stainless steel tube	10-20 nm	Copper-water	X-ray diffraction spectrum	37	50
[32]	2006	Ni-Cr wire	85 nm	Titania-water	SEM	NA	Enhanced
[33]	2007	Cu block	30 nm	CuO-water	TEM	NA	50
[60]	2008	Cu block	50 nm	CuO-water	NA	25	Enhanced
[61]	2010	Copper surface	15 nm	CNT-water	TEM	NA	63
[67]	2012	Stainless steel	NA	Al_2O_3-water	SEM	NA	212
[48]	2011	Platinum	10 nm	γ-Fe_2O_3-water	SEM	30	Enhanced
[34]	2010	Plate stainless steel	1.91 μm	Diamond	DLC	70	11
[23]	2010	Copper block	139 nm	Al_2O_3-water	NA	30	Enhancement
[29]	2011	Nickel	110 nm	TiO_2-water	SEM	16	82.7
[35]	2011	Copper block	30 nm	Silica-water	SEM	NA	Enhanced
[36]	2013	Nichrome wire	10 μm	Silica-water	SEM	37	250
[62]	2014	Stainless steel	100 nm	SiC-water	SEM	NA	105
[37]	2012	Ni-Cr	50 nm	Fe_3O_4/ethylene glycol, water	SEM	65	100
[52]	2013	Stainless steel plate	50-90 nm	ZnO-water	DLS	NA	Enhanced
[53]	2013	Copper plate	NA	Alumina-water	SEM	70	Enhanced
[38]	2012	Copper	45 nm	Al_2O_3-water	DLS	35	Enhanced
[54]	2010	Stainless steel plate	10 nm	Copper-water	AFM	57	48
[39]	2012	Ni-Cr	30±5 nm	magnetite/water	SEM	NA	70
[40]	2013	Copper	40 nm	Al_2O_3-water	AFM	NA	Enhanced
[68]	2014	Ni-Cr	47 nm	TiO_2-water	SEM	NA	Enhanced

→

Table 2. Continuation

Ref.	Year	Heating surface	Particle size	Nanofluid	Surface analysis	ΔT [°C]	CHF enhancement [%]
[55]	2011	brass	45 nm	SiO_2-water	XRD	NA	Enhanced
[56]	2011	brass	20 nm	SiO_2-water	NA		Enhanced
[63]	2013	Stainless steel plate	70 μm	ZnO-water	NA	30	Enhanced
[59]	2012	Copper plate	21 nm	TiO_2-water	NA	NA	Enhanced
[57]	2012	Copper plate	25 nm	TiO_2-water	SEM	35	1.8
[41]	2014	Ni-Cr	50 nm	Alumina-water	NA	NA	Deteriorate
[42]	2014	Copper plate	200-500 nm	GON-water	TEM	80	Enhanced
[43]	2014	Ni-Cr wire	23-37	CuO-water	NA	NA	90-160
[50]	1994	Copper block	NA	FC-72	SEM	26	Enhanced
[64]	2015	Copper	21 nm	TiO_2-water	NA	20	Enhanced
[44]	2013	Ni-Cr wire	30 nm	Al_2O_3-water	NA	NA	Enhanced
[65]	2009	Copper plate	25 nm	Alumina-water	NA	30	Enhanced
[48]	2011	Platinum	100 μm	γ-Fe_2O_3-water	SEM	30	Enhanced
[66]	2013	Copper plate	85.3 nm	TiO_2-water	TEM	40	Enhanced
[45]	2013	Ni-Cr wire	NA	GO-water	NA	NA	320
[46]	2005	NiCr	50 nm	Silica-water	NA	50	10-15
[49]	2010	NA	>45 μm	GO-water	SEM	NA	179
[47]	2014	Ni wire	>45 μm	GO-water	TEM	NA	Enhanced
[58]	2015	Copper	NA	FC-87	NA	NA	37

Figure 7 describes the nanofluids type with their variation on CHF. It is clear from the figure that grapheme particle in water enhances more heat as compare to any other nanoparticle.

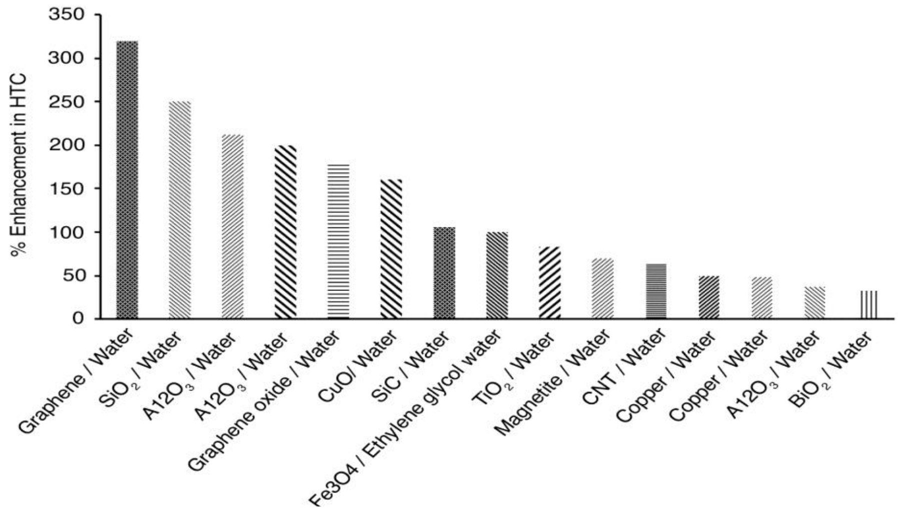

Figure 7. Comparison of CHF enhancement for different nanofluids

Experimental study on HTC

This section is divided into three sub-section based on the shape of heat conducting channel to boil nanofluid

Boiling of nanofluids through circulate plate heater

The set-up most commonly used by the previous researchers for pool boiling consists of a heating device which is usually mounted at the bottom of the heating block. The vessel is completely insulated and heat is transferred through one direction conduction from plate. A sample of circular plate heat transfer assembly used by [69] is shown in fig. 8.

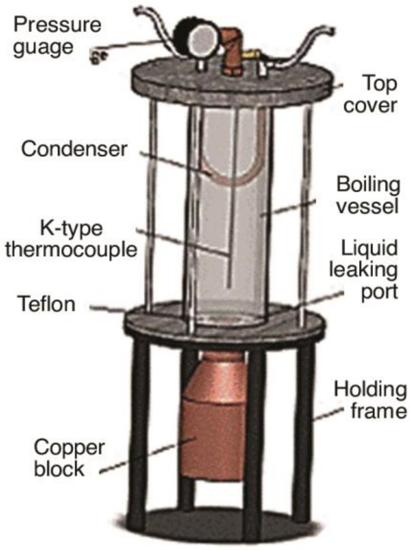

Figure 8. Experimental apparatus used by [68]

Boiling heat transfer is significantly enhanced by using nanoparticles in base water. On the other hand increasing particle loading to 1.35% by weight, heat transfer enhanced and reached up to almost 40%. The particle size used was 10-15 μm [70]. Solid dispersion at low volume fraction ZrO_2-water nanofluid results high heat transfer and by increasing solid concentration heat transfer decreases. On the other hand addition of surfactant increases heat transfer and this addition gives drastic deterioration in heat transfer [71]. Boiling heat transfer experiment on horizontal flat square copper surface using δ-Al_2O_3 nanoparticle were conducted. Refrigerant R141b at (0.001-0.1 vol.%) concentrations with and without surfactant sodium dodecyl benzene sulphonate (SDBS). Average size of nanoparticle used was 20 nm given by SEM. Authors found that at 0.01 vol.% boiling heat transfer decreases with addition of SDBS whereas at 0.1vol.% and 0.001vol.% concentrations, boiling heat transfer increases by adding SDBS [72].

The TiO_2 nanofluid with concentration ranging from 0.0005, 0.0001, 0.005, and 0.01 vol.%. was used to enhance heat transfer. Transmission electron microscopy confirms the average size of copper nanoparticle as 21 nm. Copper and aluminium surfaces with different roughness values were used for heating. Authors concluded that higher nucleate pool boiling coefficient was obtained at 0.0001 vol.% using copper heater surface. On the other hand HTC decreases by increasing the concentration from 0.0001 vol.% [73]. Al_2O_3-water nanofluid at different concentrations (0.01, 0.1, and 0.5 vol.%) on a horizontal flat copper surface were tested. Size of alumina particle was in the range of (40-50 nm). They found that highest HTC resulted from highest concentration of nanofluid into base fluid [74]. Addition of nanoparticle on heating surface creates a layer which effects boiling heat transfer. The ZnO nanoparticle with size of 40 nm were experimented with and without base fluid. They observed that after four cycles of test, performance of water increases to 62% as the concentrations of nanoparticle increases to 24% as compared to water on a clean surface. The heat transfer decreases with the creation of nanoparticle layer on the surface. [75]. Silver nanoparticle was used to enhance pool boiling heat transfer at atmospheric pressure. Cluster deposition and hydrophobicity increases with increasing nanoparticle concentration whereas deposition stability decreased. Authors observed that CHF increases up to 196 W/cm^2 which was120% higher than water used as a fluid. They concluded that compared to the polished copper surface, inclination and re-entrancy of surfaces enhanced pool boiling performance [76]. Variation of HTC *vs*. heat flux is shown in fig. 9.

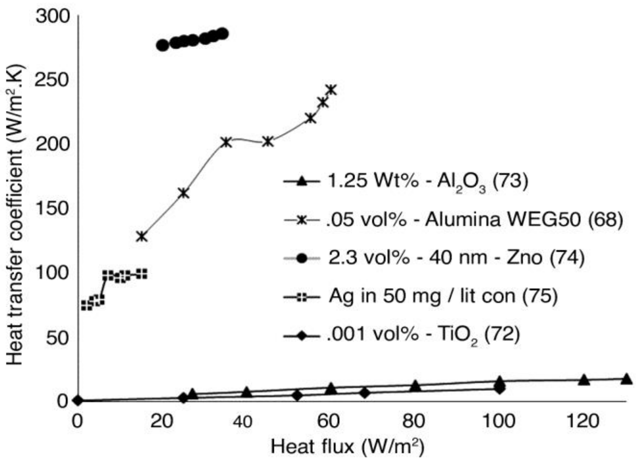

Figure 9. The HTC *vs*. heat flux for different nanofluids

Boiling of nanofluid through square plate heater

In this method heat is provided to nanofluid through a plate heater through conduction. Mostly copper electrodes used as a heat resistivity source to heat the plate. An experimental set-up used [54] is shown in fig 10.

To find the effect on HTC stainless steel test specimen with TiO_2-water nanofluids were used. The DLC shows that average size of nanoparticle was in-between 4-10 nm. Pool boiling with TiO_2 coated surface, deterioration up to 50% has been observed due to adhesion energy [77]. Nanostructured surface (NSS) coating on platinum wire was attained by the addition of charged γ-Fe_2O_3 nanoparticle on platinum wire. Scattering electron microscope was use to ensure the size of nanoparticle as 10 nm. Decrease in HTC was observed when the wire was entirely covered with nanoparticle [48]. Al_2O_3/Water nanofluid was experimented on copper mini-channel wire. Size of nanoparticle was measured by scattering electron microscope. Boiling heat transfer increases with the generation of nanoparticle coating on heater surface [23]. Al_2O_3-water and SiC-water nanofluids having volume concentrations of 0.01%, 0.1%, 0.5% and 1% were experimented. Scattering electron microscope was used for size measurement. Nanofluid effects heavily depend on concentration, size, material and foam structure [78]. Alumina-water nanofluid on copper surface was experimented. Average size of particle was 45nm as given by DLS. Increasing the boiling surface area using alumina as nanoparticle decreases the boiling HTC. Authors observed that this reduction is due to conductive resistance increment and blocking of active nucleation cavity [38].

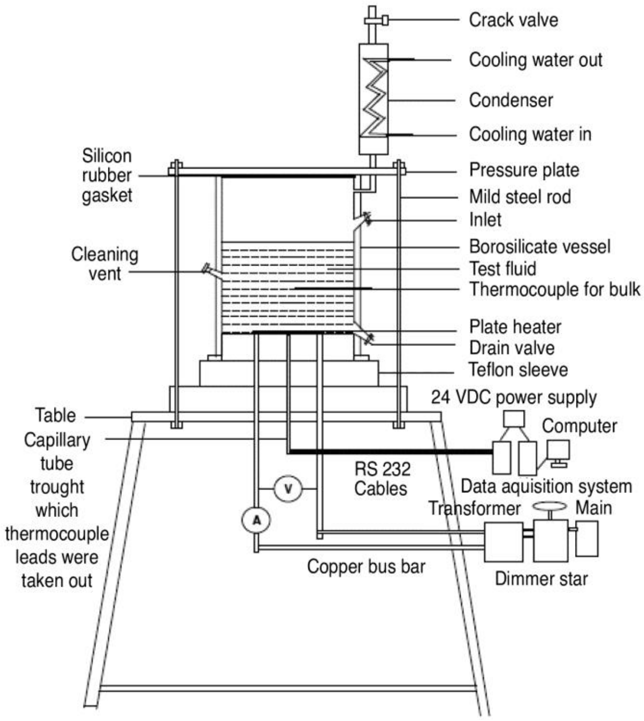

Figure 10. Experimental apparatus used by [9]

Charged γ-Fe_2O_3-water nanofluid was used for the enhancement of heat transfer with 100 μm platinum wire at 1 bar. Average nanoparticles sizes were 40 nm and 50 nm as measured by transmission electron microscope. It was concluded that enhancement in heat transfer is 70% when nanoparticle loading was 0.5% [48]. Copper-water nanofluid having average size of 10 nm was used for pool boiling heat transfer enhancement. The HTC decreases with copper-water nanofluids. This coefficient has a decreasing trend with nanoparticle concentration. On the other hand CHF of pure water was decreased by 75%, 68%, and 62% for 0.25%, 0.5%, and 1.0% if copper nanoparticles are dispersed in water with surfactant nanofluids, respectively [54]. Four different copper test chips of graphene and GO with coated thickness 1 μm, 2 μm, 3 μm, and 4 μm were inserted on heating surface. Hydrophobic wetting behaviour was shown from contact angle which was measured from coated surface. Authors observed that as compared to plain uncoated chip, copper chip thickness of size 1 μm shows 42% more enhancement in HTC. They reported that highest heat transfer enhancement was obtained with thinnest coated chip [79]. Nucleate pool boiling experiments were performed for the heat transfer enhancement with RGO colloids in water base liquid. They used four different percentages (0.001, 0.005, and 0.0010 wt.%) of RGO in base fluid. Formation of RGO flake layer is responsible for the decrease of boiling heat transfer with increasing concentration of nanoparticle [80].

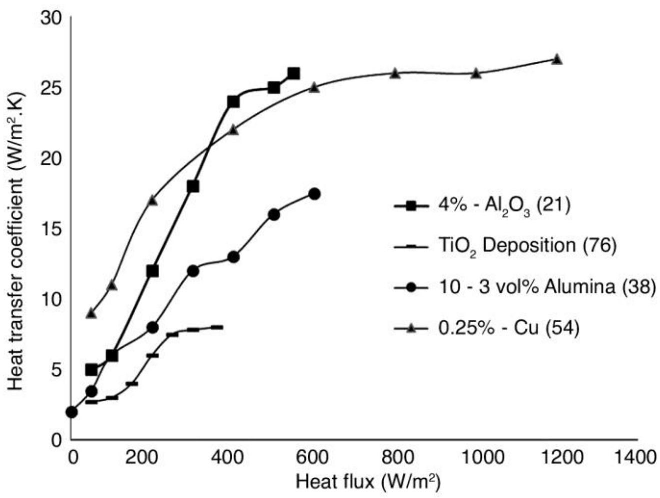

Figure 11. The HTC *vs.* heat flux for different nanofluids

The Al_2O_3-water ethylene glycol nanofluids with different volume concentration were used at atmospheric pressure. At 0.75 vol.% nanoparticle HTC increases to 64%. This increment in HTC was due to the change in heated surface status [81]. Figure 11 shows the change in HTC with heat flux when square plate is used for heating.

Boiling of nanofluid through Rod/tube

In this type of experimental set-ups, to boil nanofluid, a heating module mostly located at the bottom inside of the test chamber consists of power input electrodes, a resistive wire heater with provision of steady state current. Experimental apparatus presented at fig. 12, a simple wire heater pool boiling set-up, was used in [34].

The CuO and ZnO nanofluids were examined for pool boiling heat transfer with sodium dodecyl sulphate (SDS) as a surfactant. Addition of SDS increases the boiling performance. Authors reported that 0.01wt.% of CuO was the optimum value of surfactant concentration with CuO which gives maximum heat transfer [82]. An experimental study was carried out with γ-Al_2O_3/water and SnO_2/water Newtonian nanofluids. Average sizes of γ-Al_2O_3 and SnO_2 were 20-30 nm and 55 nm, respectively. These nanofluids increase HTC notably than the base fluid due to type and concentrations of nanoparticles [83]. The TiO_2 nanoparticle with refrigerant R141b at 0.01, 0.03, and 0.05 vol.% were experimented. It was reported that nucleate pool boiling heat transfer is deteriorated and at 0.05 vol.% boiling heat transfer was suppressed [84].

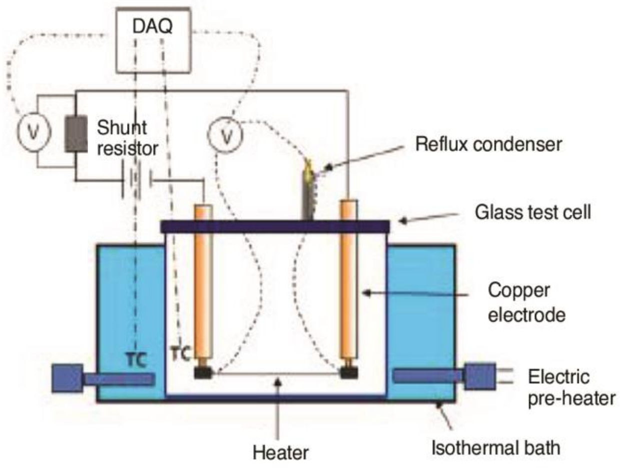

Figure 12. Experimental apparatus used by [34]

An experimental study was performed using Cu-distilled water nanofluids. Transmission electron microscope confirms the size of nanoparticle as 122 nm. A maximum increment of about 15% was observed at 0.5 wt.% of Cu when added in distilled water at 30 C°. Authors reported that thermal resistance is directly proportional to load [85]. There exists an inverse relation between carboxy methyl cellulose/γ-Al_2O_3 concentration and HTC. On the other hand nanparticle (γ-Al_2O_3) concentration increases the heat transfer. Boiling HTC increases to about 25% at nanoparticle 1.4 wt.% [86]. The TiO_2-water nanofluids were experimented on nickel with 110 nm. Authors concluded that boiling HTC increases with TiO_2-water nanofluids as compared to water [29]. Experiments were conducted on copper tube using Silica-water nanofluids at atmospheric and sub-atmospheric pressure. The HTC slightly increased with functional nanofluids which changed thermo-properties of surface [35]. For smooth surface (Ra~25 nm) nucleate boiling heat transfer using alumina nanoparticle increases but for rough surface (Ra~420 nm) it remains unchanged. Particle deposition effect can be reduced by proper surface engineered nanoparticles [87]. The Al_2O_3-water nanofluid with nanoparticle having an average size of 20-150 nm was used on brass surface. The HTC increases with nanofluids having smooth surface. Size of particle, geometry of surface and their interaction affects heat transfer [88]. The TiO_2/R141b-ethyl glycol nanofluid was experimented on brass surface to enhance the HTC with 21 nm nanoparticle size. Increasing the particle volume concentration decreases heat transfer. This decrement in heat transfer is mostly affected at high heat flux, whereas it increases at high boiling pressure [89].

The CuO-water nanofluid experiments were conducted at different volumetric concentrations (0.1-0.4%) having 50 nm nanoparticle size. Thermal resistance of surface was intensified due to thick layer of nanoparticle on the surface which deteriorated the HTC [90]. Convection and nucleate boiling heat transfer was the two different heat transfer region for dilute stabilized Al_2O_3 ethylene glycol nanofluid. Secondly heat flux and pool boiling HTC have a direct relation [91]. Plain and NSS were experimented with three different fluids. Authors concluded that with pure water boiling conditions nucleate boiling HTC (NBHTC) was increased on the plain surface (PS), but decreased on the NSS. Authors observed that NBHTC was strongly affected by chemical reaction between heater surface and fluids [92]. Heat transfer can be affected by using different anodizing techniques to obtain nanoporous structure. Alumina sponge-like nanoporous structure was used with self-assembled monolayer (SAM) to improve the number of activation site density. Authors found that this combination substantially enhanced the HTC [93]. Authors proposed mechanistic model – with the combination of forced-convection and thin liquid film evaporation which was given as:

$$q" = \frac{\pi d_b^3}{6} N_a^{'} f_b i_{lv} \rho_v + \left(\frac{\Delta T}{C_q} \right)^{1/y} N_a^{1/y} + \frac{C K_l \delta \Delta T}{1 - \cos\theta} N_a^{1/y} \tag{3}$$

To investigate the effect of SDS, three different water based coolant namely nanoalumina, nanosilica, and nanozinc oxide were used with and without using SDS. Stainless steel was used as a test specimen. Authors reported that addition of SDS decreases heat transfer. They also resulted that best coolant for heat removal is nanozinc oxide and SDS mixture [94]. The Al_2O_3-water nanofluid was used with Ni-Cr heater to enhance pool boiling heat transfer. Transmission electron microscopy's results confirmed the average size of nanoparticle as 47-150 nm. Authors found that with rough heater (R_a-524 nm) HTC enhanced and this enhancement is 70% at 0.5 wt.%. They reported that HTC decreases with decreasing surface roughness [95]. Figure 13 shows the variation in heat flux with HTC when electric rod is used for boiling.

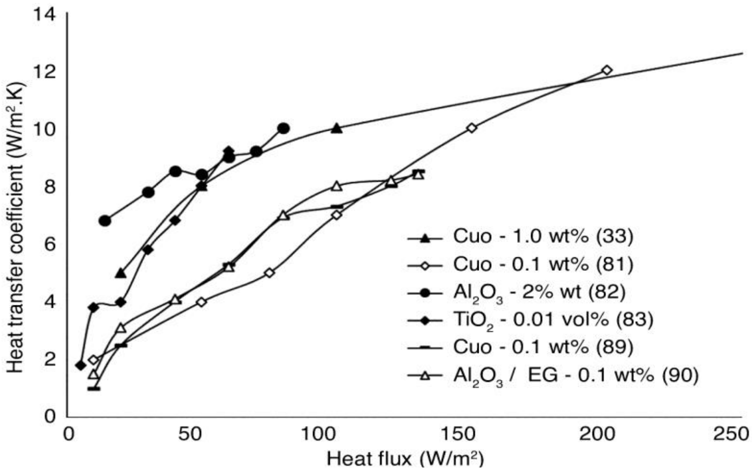

Figure 13. The HTC *vs.* heat flux for different nanofluids boiling using rod heater

Effect on HTC using nanofluids has been discussed in this section. According to [29, 38, 69, 71, 73, 81-84, 90] HTC increases with increasing nanoparticle in base fluid. After an experimental investigation [72] pointed out that addition of surfactant with nanofluid increases heat transfer.[23, 38, 48, 68, 74, 89] concluded that addition of nanoparticle to base fluid generates a surface layer on heating surface which decreases heat transfer but [78, 80] pointed out that this layer increases heat transfer. Experimental investigation of [72, 75, 94] rough surface pool boiling using nanofluid increases heat transfer as compared to polished and smooth surface but [86, 87] pointed out that heat transfer increases with smooth surface. In [40] does not give any results on either surface but pointed out that surface affects heat transfer. There are some researchers [54, 79, 88, 93] whose results pointed out that addition of nanoparticle to base fluid for pool boiling decreases heat transfer. According to [21] natural convection does not affect heat transfer. In [77] concluded that nanoparticle effect on heat transfer depends on concentration of nanofluid and size of nanoparticle. Experimental results of [35, 92] pointed out that changing behaviour of thermophysical properties is the main reason behind enhancement in heat transfer. Heat transfer depends upon contact angle between pool boiling surface and nanofluids [91].

Reasons for increase/decrease in boiling HTC

According to published papers thermophysical properties has a major role on boiling HTC. It has been observed that major role of nanoparticle is on thermal conductivity and surface tension whereas viscosity, density and heat capacity remains nearly constant. Commonly used heat transfer fluids have less thermal conductivity than that of nanofluids [23]. Large specific surface area due to small particle size and interfacial liquid layering are the main reasons to increase the effective thermal conductivity [31]. Increase in thermal properties is responsible for increase in boiling HTC [70]. The thin layer formed on the heating surface is very important in conduction heat transfer and boiling HTC is strongly related to thermal conductivity [83]. Nanoparticles increase the convection heat transfer when suspended in base fluid due to nanoparticle migration and chaotic movement. Also turbulence flow increases heat transfer [69]. Surface tension of the fluid decreases due to suspension of nanoparticle in it which decreases the formation of bubble and active nucleation sites which increases boiling HTC [35].

Not only thermal conductivity and surface tension are affected by the presence of nanoparticle but also surface properties of boiling surface are altered by presence of nanoparticle which also increases boiling HTC [24]. Modified surface topology is main reason behind enhancement in boiling HTC rather than deviation in thermophysical properties [63]. Vapour bubbles grow on boiling surface during nucleate pool boiling. Nanoparticle are accumulated on the heating surface when these vapour bubbles are departed from heating surface. Amount of settled nanoparticles enhance boiling HTC. Heat transfer negatively disturbs sedimentation on heating surface as nanoparticle concentration increased or reached to an optimum value. Increased thermal resistance between heating surface and fluid is the possible reason for this deterioration due to several orders of magnitude of thermal conductivities of oxide nanoparticles [70]. Deposition of nanoparticle works against the bubble growth as it is horizontal component of surface tension often called as adhesion energy. In this way bubble emission frequently decreases as heating surface is being covered with more bubbles. Moreover boiling HTC decreases due to active nucleation sites as liquid wets the nanoparticle coating surface completely. Reversely capillary wicking effect is responsible for enhancing heat transfer which sucks the liquid [63]. Generation of new activation sites is responsible for increase in surface roughness which enhances boiling HTC. Variation in surface structure occurs due to nanoparticle deposition because of high particle concentrations [59]. Heating surface is covered by a porous surface due to nanoparticle in case of higher nanoparticle deposition. Depending upon either original surface condition or size of nanoparticle surface roughness can be increased [21] or decreased [33]. Surface roughness increases if surface roughness is smaller than nanoparticle. If surface roughness is higher than nanoparticle it will decrease [17]. Boiling HTC decreases at higher heat flux while at lower heat flux this value can be negligible. This is because at low heat fluxes large voids are generated whereas smaller cavities are generated at higher heat flux. In case of nanofluid boiling these cavities are filled with nanoparticles so activation site decreases which decreases HTC [31]. The HTC variation with various parameters is shown in tab. 3.

It is clear from the fig. 14 that HTC is maximum when carbon nanoparticles are used for boiling and minimum when ZnO particle used in water for heating.

Table 4 describes the HTC variation with temperature difference given by various researchers.

Table 3. Parameter variation effects on HTC

Parameter variations	Reason	Effect on HTC
Surface tension decrement	Decrease in bubble radius and increase in number of activation sites	Increase
Heat flux increases	Due to small cavities filled with nanoparticle number of activation site decreases	Decrease
Thermal conductivity increases	Due to conduction heat transfer increment	Increase
Suspension Stability increases	Agglomeration decreases	Increase
Fluid turbulence increase	Increase in convection heat transfer	Increase
Particle concentration increases	Deposition of nanoparticle increases	Decrease

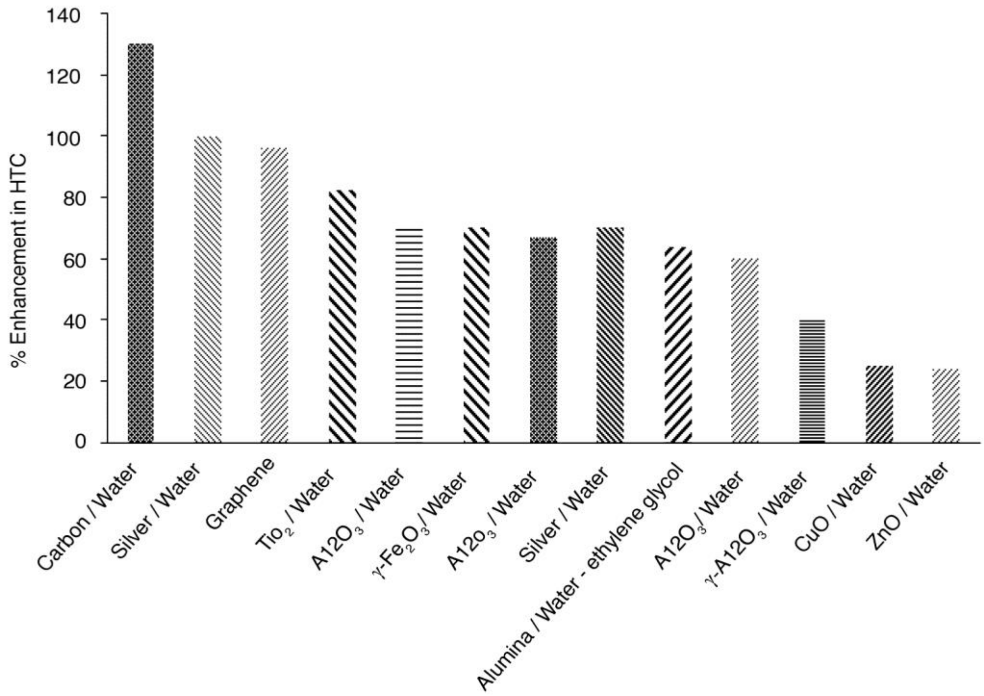

Figure 14. Comparison of enhancement of HTC different nanofluids

Effect of thermophysical properties of nanofluids used in pool boiling

This section gives the effect of thermophysical properties on HTC and CHF of nanofluids in pool boiling.

Viscosity

Viscosity of nanofluids has core importance. Following equation can be used to find the viscosity of nanofluids [96]:

$$\mu_{\mathrm{nf}} = \mu_{\mathrm{bf}}\left(1+1.25\Phi\right) \tag{4}$$

Table 4. Summary of the pool boiling experiments and their effect on HTC

Ref.	Year	q [kwm^{-2}]	Heating surface	Particle size	Nanofluid	Surface analysis	ΔT [°C]	HTC [%]
[70]	2005	120	Stainless steel	10-15 µm	γ-Al_2O_3-water	SEM	10	40
[21]	2005	500	Copper	47 nm	Al_2O_3-water	TEM	21	Deteriorate
[71]	2008	NA	Copper	20-25 nm	ZrO_2-water	TEM	23	Enhanced
[33]	2007	NA	Stainless steel	30 nm	CuO-water	TEM	NA	25
[61]	2010		Copper	15 nm	Carbon-water	TEM	NA	130
[82]	2013	350	Stainless steel	NA	CuO-water	FESEM	19	Enhanced
[83]	2009	80	NA	20-30 nm	γ- Al_2O_3-water	NA	11	Enhanced
[72]	2014	NA	Copper	20 nm	δ- Al_2O_3-water	SEM	25	Enhanced
[84]	2009	70	Copper	NA	TiO_2-water	TEM	11.5	Deteriorate
[85]	2013	NA	Aluminum	122 nm	Cu-water	TEM	NA	Enhanced
[77]	2010	380	Stainless steel	4-10 nm	TiO_2-water	DLS	NA	Degrades
[48]	2011	NA	Platinum	10 nm	γ-Fe_2O_3-water	SEM	30	Enhanced
[23]	2010	NA	Copper	139 nm	Al_2O_3-water	NA	30	Enhanced
[29]	2011	1100	Nickel	110	TiO_2-water	SEM	17	82.2
[35]	2011	650	Copper	30 nm	SiO_2-water	SEM	NA	Enhanced
[78]	2014	NA	20nm	20 nm	Al_2O_3-water	SEM	15	Deteriorate
[87]	2012	NA	Copper	20-150	Al_2O_3-water	NA		Enhanced
[88]	2011	NA	Brass	20-150 nm	Al_2O_3-water	NA	8	Enhanced
[74]	2012	NA	Copper	40-50 nm	Al_2O_3-water	NA	27	Enhanced
[38]	2012	600	Copper	45 nm	Al_2O_3-water	DLS	36	enhanced
[54]	2010	1000	Stainless steel	10 nm	Copper-water	AFM, XRD, TEM	55	Enhanced
[40]	2013	NA	Copper	40 nm	Al_2O_3-water	AFM		enhanced
[55]	2011	NA	Brass	34 nm	SiO_2-water	XRD	110	Enhanced
[89]	2014	NA	Brass	21 nm	TiO_2/R141b-ethyl glycol	NA	120	Deteriorate
[90]	2015	NA	Stainless steel	50 nm	CuO-water	SEM	120	Deteriorate
[91]	2014	NA	Stainless steel	45-50 nm	Al_2O_3/ethylene glycol	TEM	100	Deteriorate
[69]	2013	600	Copper	20-30 nm	Al_2O_3-water-ethylene glycol	TEM	16	64
[95]	2007	60	Ni-Cr	47-150 nm	Al_2O_3-water	TEM	11	70
[48]	2011	NA	Platinum	47 and 150 nm	γ-Fe_2O_3-water	TEM	28	70
[94]	2016	NA	Stainless steel	0.15 µm	γ- Al_2O_3-water	AFM	20	Deteriorate
[79]	2017	NA	Copper	1 µm	Graphene	SEM	NA	96
[96]	2016	NA	Silicon oxide	0.675 nm	GO	TEM	NA	Enhanced
[81]	2013	NA	NA	50 mm	Al_2O_3-water	NA	22	67
[93]	2012	100	Al 6061	NA	Al_2O_3-water	SEM	10	60
[75]	2010	32	Stainless steel	40 mm	ZnO-water	AFM	NA	24
[76]	2017	NA	Copper	20 nm	Silver-water	TEM	NA	100

Those particles which do not have any surface charge but under predicts the viscosity can be calculated using equation (4). By incorporating the electro-visco force, the equation can be modified:

$$\mu_{\rm nf} = \mu_{\rm bf}\left(1+10\Phi\right) \tag{5}$$

Viscosity of nanoparticle decreases with the increase in temperature and increases with nanoparticle concentration. In [70, 97, 98] it is concluded that classical model and low volume fraction estimation of viscosity was found to be good, burt fails as the temperature varies [99]. Increasing concentration kinematic viscosity of nanofluids increases. This is because during electro stabilization process, electro viscous force is induced in nanofluids [81]. Viscosity of nanofluids increases with particle concentration and decreases with temperature. Shear rate also enhances viscosity. Authors have concluded that we could not use this as a tool for deterioration in pool boiling heat transfer [17]. On CHF enhancement, effects of viscosity reported a minimal difference between pure water and nanofluid. They concluded that it can be due to low concentration of nanofluids used in their study [23]. According to [100] for the tested concentrations of nanofluids, it is found that viscosity data are similar to that of pure water. Variation of viscosity with temperature is shown in fig. 15.

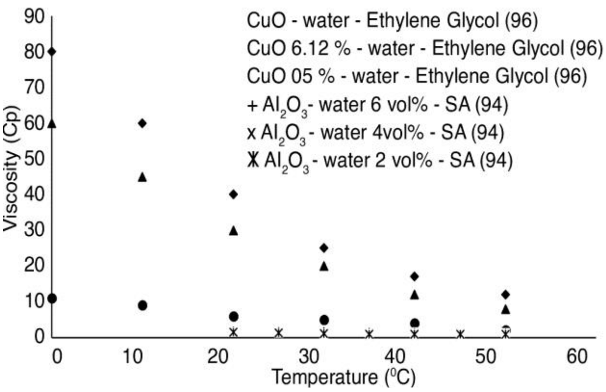

Figure 15. Viscosity variation with temperature

It can been seen from fig. 15 that viscosity increases as temperature, in pool boiling, decreases but as temperature increases viscosity decreases and this trend is seen in almost all the nanofluids. Value of viscosity becomes zero at higher temperature.

According to [100] and [23] viscosity of nanofluids and water has similar behaviour with temperature changes but [17, 70, 81, 97] reported that by increasing the particle concentration, viscosity of nanofluids increases and decreases with increasing temperature.

Surface tension

Just like the thermal conductivity in present years surface tension also has also an important role in the enhancement of CHF of the nanofluids.

Gas- liquid surface tension depends on nanoparticle size and concentration. The 2.5 and 10.4 nm diameter nanoparticle diameter was tested. When the nanoparticle size was 2.5 nm largest reduction in surface tension exists. As nanoparticle concentration increases, surface tension also increases [101]. Relaxation of surface tension is the main factor for the delay in the occurrence of CHF of CNT nanofluids. However to maximize the heat flux to recognize the optimum CNT and surfactant concentration needs to be worked upon [102]. Nanoparticle surface tension variation with particle concentration is given by [101] shown in fig 16. In general, just like concentration, as temperature increases surface tension decreases.

It can been seen from the fig. 16 that value of surface tension is high at low concentration of nanofluids. Surface tension decreases as concentration have an inverse relation up to certain limit after which this effect has not been seen.

According to [100] as concentration increases, surface tension also increase but [101] pointed out that delay in CHF, especially for carbon nanotubes, is due to relaxation of surface tension. In general as temperature increases surface tension decreases just like concentration increases surface tension increases.

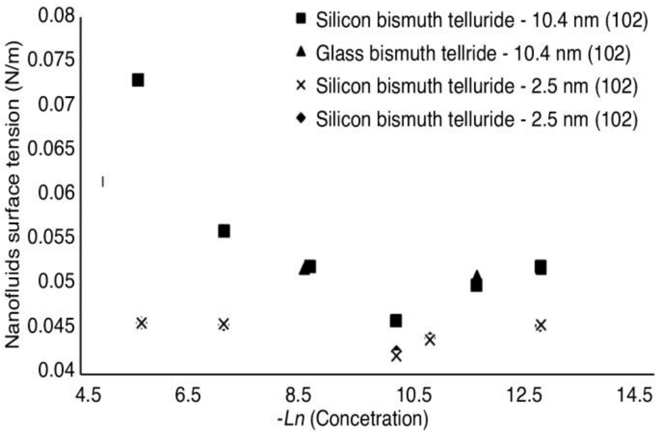

Figure 16. Variation of effective surface tension with nanofluid concentration [102]

Quenching

Quenching is very important whenever there is rapid solidification and heat treatment in nuclear reactor. Quenching occurs when a high temperature system/job is cooled quickly. All boiling mechanisms can be observed in quenching process. Fewer studies for the quenching behaviour of nanofluids have also been conducted. Experiments were conducted on silver sphere with 10 mm diameter using Ag and TiO_2 nanoparticle in water based nanofluids. It is found that there is a quick quenching of hot sphere due to vapour film forming around it. Hot sphere quenched more rapidly through nucleate boiling than film boiling [103]. Experiments were conducted with SiO_2-water nanofluids which quench a vertical cylinder for the pool boiling heat transfer experimentation at saturation temperature and atmospheric pressure. Four different concentrations (0.001, 0.01, 0.05 and 0.1 vol.%) of SiO_2-water and pure water were used as a coolant. It is investigated that cooling behaviour of SiO_2 water nanofluid and pure water is similar. Boiling heat transfer decreases in nucleate pool boiling region as compared to pure water due to deposition of nanoparticle [55].

Increasing the GON nanofluid concentration, static contact angle shows the variation of surface wettability in the investigation of transient pool boiling of aqueous nanofluids with GO nanosheets [42]. Experimental investigation was carried out with CNT of various sizes for the quenching of hot stainless steel. Different sizes of multi-walled carbon nanotubes (MWCNT) ranging from 1 μm to 5 μm in length with 30 μm to 60 μm in diameter were used. The concentrations of MWCNT were fixed as 0.5%. They found that due to discrepancy in the sizes of CNT in nanofluids CHF and Leidenfrost point (LFP) are enhanced. They reported that most significant effects on boiling behaviour were observed with 5 μm length and 60 μm size CNT [104].

According to [102] hot spheres quenched more rapidly due to vapour film formed around them as compare to sphere having no film. In [55] concluded that quenching behaviour of sphere is same in both water and nanofluids and boiling heat transfer decreases in nucleate pool boiling region. In [42] reported that formation of microlayer is main reason for enhancement of CHF in quenching. In [103] reported that discrepancy is the core reason in the enhancement of both CHF and LFP which is due to the sizes of nanoparticle in nanofluids.

In summary, influence of thermal transport properties has not played any vital role on the delay in the occurrence of CHF. However, at low concentration, these were observed to plays a role. Therefore, with low volume fraction and smaller size in particle for further investigation of their properties is needed to make conclusive statement on the CHF enhancement.

Other effects

The HTC enhances using the SiO2-water nanofluid as a coolant in miniature plate fin heat sink. Aspect ratio and HTC are directly proportional to each other [105].

Three different nanofluids namely Al_2O_3-water, TiO_2-water, and CuO-water used in circular channel having 400 μm diameter and block dimension 10 mm ×10 mm × 4 mm. CuO-water nanofluids showed significant increase in thermal performance as compared to Al_2O_3 and TiO_2. Authors observed that 13.15% enhancement in heat flux occurred at 4 vol.% of CuO water nanofluids [106]. An experimental investigation was carried out using low concentrations (<1 g/l) of nanofluids. Nanoparticle deposition on heater surface increases heat transfer [23]. Trapezoidal micro-channel has inferior efficiency to triangular micro-channel but superior to rectangular SiO_2-EG nanofluids have highest Nusselt number. As diameter of nanoparticles increases Nusselt number decreases. On the other hand Nusselt number increases with volume fraction [107]. Experimental investigation was carried out on bare and scale small diameter wire at earth gravity conditions. Calcium carbonate was used as a scale deposition on both wires. Authors concluded that NBHTC was same at both microgravity and earth gravity conditions. Scale wire gives higher CHF as compared to bare wire [108]. Hydrophilic and hydrophobic patterns on smooth and flat surfaces enhance heat transfer. They found that CHF and heat transfer enhancement of the enhanced surfaces were 65% and 100% higher respectively when compared to hydrophilic surface when the wetting angle is 7° [109]. Hydrophobic and hydrophilic regions are shown in fig 17.

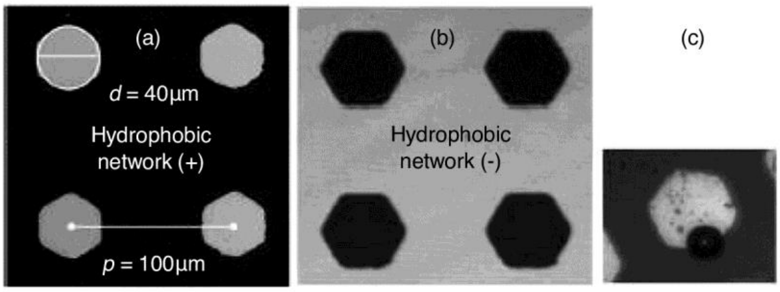

Figure 17. Typical micrographs (a) and (b) of surfaces with hydrophilic black and at low superheat, bubbles typically nucleate at the interface between areas of different wettability (c)

Experiments were conducted on vertical and inclined mini-channel configurations on copper surface. Surface with more depth and high surface augmentation reached a maximum heat flux of 150 W/cm^2, whereas CHF enhancement of 65% was seen over a PS [110]. The TiO_2-water nanofluid was used to enhance pool boiling heat transfer. The TiO_2 nanoparticle improves the surface wettability as compared to clean surface [77]. An experimental investigation was carried out with γ-Fe_2O_3-water nanofluid. Deposition of nanoparticle on platinum wire γ-Fe_2O_3 improves surface wettability [48]. An experimental investigation was carried out with Al_2O_3-water nanofluid on 10 mm plain copper heater. Authors reported that deposition of alumina particle creates a layer on heating surface which improves surface wettability [53]. An experimental investigation was carried out with alumina/water nanofluid with .01 vol.%. Increased wettability and hydrodynamic instability changes CHF value [41]. Boiling heat transfer and CHF is affected by surface deposition of SiO_2/water nanofluid. Deposition of nanoparticle on the heating surface changes the quenching process. This increases surface wettability and CHF [55].

The Al_2O_3-water nanofluid with Ni-Cr wire heater was analysed. Decrease in porosity increases CHF [41]. Average roughness of surface is dramatically deteriorated by increasing the concentrations of nanofluid in base fluid [91]. Experiments were conducted on horizontally oriented surfaces to check their effects on enhancement of heat transfer. Authors concluded that as surface roughness changes the CHF also changes. When the roughness value becomes 6 CHF values reaches almost to 208 W/m^2 [111]. Experimental investigation was carried out with TiO_2 nanoparticle for the relation between CHF enhancement and macro layer creation on heater surface. Creation of thicker micro layer due to deposition of TiO_2 increases heat transfer [57]. Experimental investigation was carried out with Al_2O_3-water ethylene glycol nanofluid. Authors reported that thicker macro layer is formed due to the higher concentrations of nanofluids on heating surface [69]. Bare and fouled wire is used to enhance boiling heat transfer. Calcium carbonate was used as a scale deposition on both the wires. For earth gravity, when the heat flux was same for both wires, vigorous bubbling was observed on the fouled wire compared to that on the clean wire [108]. Using Al_2O_3 and Fe_3O_4 base water, bubble frequency increases approximately two times as compared to pure water. This bubble frequency reverted hot spots on heating surface [44]. Cumulative density of active nucleation sites varies as q^2 irrespective of the degree of wettability of the surface [112]. Addition of nanoparticle concentration in base fluids can increase the thermal conductivity of any base fluid. An experiment was conducted with 50 vol.% water and 50 vol.% ethylene glycol with functionalized single walled carbon nanofluids (F-SWCNF). Different volume concentrations (0.025, 0.055, 0.08, 0.0125, 0.25, 0.53, and 0.65%) of F-SWCNF were used for suspension. Authors concluded that comparing the oxide nanofluid of alumina/water-EG (50:50 vol.%) with SWCNF, it was observed that SWCNT have superior thermal conductivities. On the other hand by adding 0.65% SWCNTs to the EG-water solution at 50 °C, thermal conductivity increased up to 52.7% [113].

Correlations used by different researchers for pool boiling

This section gives some of the basic correlations used to find out the CHF and HTC of water and nanofluids used in pool boiling.

Table 5. The HTC and CHF correlations

Ref.	Correlation	Surface
[114]	$q''_{CHF,Z} = 0.131 h_{lv} \rho v^{\frac{1}{2}} [g\sigma\,(\rho_l - \rho_v)]^{1/4}$	Square polished copper surface
[115]	$Q''_{CHF} = \dfrac{\pi}{24}\, h_{fg} \rho v^{\frac{1}{2}}\, [g\sigma\,(\rho_l - \rho_v)]^{1/4}$	When bare nickel wire boiling in water
[116]	$Q'' = \mu_l h_{fg} \left[\dfrac{g\,(\rho_l - \rho_v)}{\sigma}\right]^{\frac{1}{2}} \left[\dfrac{C_{pl}\,(T_l - T_{Sat})}{C_{hf}\, H_{fg}\, Pr_l^n}\right]^{1/3}$	When bare nickel wire boiling in water (BHT)
[117 118]	$Q''_{CHF} = C\rho_g h_{fg} \left[\dfrac{g\,(\rho_f - \rho_g)\sigma}{\rho_g^2}\right]^{1/4}$	When horizontal plate heater is used as boiling surface
[119]	$q_c = h_{fg} \sqrt[4]{\rho v^2 g\sigma(\rho_l - \rho_v)} \left(\dfrac{1 + Cos\beta}{16}\right) \left[\dfrac{2}{\pi} + \dfrac{\pi}{4}\,(1 + Cos\beta)Cos\theta\right]^{0.5}$	When functionalized nanofluids are used on smooth heated surface

→

Table 5. Continuation

Ref.	Correlation	Surface
[120]	$\frac{q_c}{h_{fg}\,\rho v^{0.5}\,[\sigma g(\rho_l-\rho_v)]^{1/4}}=0.131$	When various working fluids are used on the plain metal surfaces.
[114]	$q'_{CHF}=\frac{\pi}{24}\rho_g h_{fg}\left[\frac{g\,(\rho_f-\rho_g)\sigma}{\rho_g^2}\right]^{1/4}$	Zuber CHF correlation for pure water at 1 atmosphere pressure when Ni-Cr wire is use as boiling
[121]	$\frac{q''_{CHF}}{\frac{\pi}{24}\rho q^{1/2}h_{fg}\left[g\sigma\left(\rho_f-\rho_g\right)\right]^{1/4}}=\left(\frac{9}{2\pi}\frac{\lambda_{RT,C}}{\lambda_m}\right)^{1/2}$ $=\frac{3\left[\sigma/g\left(\rho_f-\rho_g\right)\right]^{1/4}}{\lambda_m}$ $q''_{CHF}=\frac{\pi}{8}h_{fg}\left(\frac{\sigma\rho_g}{\lambda_m}\right)^{1/2}$	Hydrodynamic instability CHF prediction model for porous heating surface
[114]	$q''_{CHF,Z}=\frac{\pi}{24}\rho_g^{1/4}h_{fg}\sqrt[4]{g\sigma\left(\rho_f-\rho_g\right)}$	When infinite upward-facing, horizontal flat plate used for heating
[122]	$\frac{q''_{CHF}}{q''_{CHF,Z}}=(1+f)^{5/16}\times\left\{\left[3^{1/2}.2\pi\left(\frac{\sigma}{g(\rho_l-\rho_v)}\right)^{1/2}\right]^2/\left(\frac{\pi}{4}d^2\right)\right\}^{1/16}$	Boiling on an upward-facing, Horizontal small disk
[123]	$q''_{CHF}=h_{fg}\rho v^{1/2}\left[g\sigma\left(\rho_l-\rho_v\right)\right]^{1/4}\left(\frac{1+\cos\beta}{16}\right)$ $\left[\frac{2}{\pi}+\frac{\pi}{4}(1+\cos\beta)\cos\left(180^\circ-\theta\right)\right]^{0.5}$	For surfaces having inclined angle (Horizontal upward facing)
[124]	$q''_{CHF}=18.684\ln(R_a)+475.29$	When surface roughness of heater surface is counted in water with contact angle
[125]	$\frac{q''_{CHF}}{q''_{CHF,Z}}=0.036\times(\pi-\frac{\pi}{180}\theta)^3R_a^{0.125}$	When surface roughness of heater surface is counted in water with contact angle
[116]	$\frac{C_{pl\Delta T}}{h_{fg}}=C_{sf}\left\{\frac{q}{\mu_l\,h_{fg}}\left[\frac{\sigma}{g(\rho_l-\rho_v)}\right]^{1/2}\right\}^{0.33}Pr_l^5$	On smooth surface when water is used as boiling fluid
[126]	$q''=\left(\frac{\pi_d^3}{6}\right)N'_a f_b h_{lv}\rho_v\left(\frac{\Delta T}{C_q}\right)^{1/y}N_a'^{\,x/y}$	When there is both porous coating on surface and forced-convection

Conclusions

A comprehensive study of the experimental results regarding the pool boiling behaviour of nanofluids presented in the literature has been reported here. Various properties including the thermophysical properties of nanofluids and the boiling surface properties, as well as their mutual interactions are the factors affecting the pool boiling heat transfer of nanofluids. Researchers have tried to explain the reasons for the contradictory results. Based on the research literature, the following conclusions are drawn.

- Increasing the nanoparticle concentration increases the Boiling HTC and CHF upto certain level beyond which boiling HTC deteriorates but does not affect CHF.
- Number of nucleate sites increases boiling heat transfer. More active cavities enhance more boiling heat transfer. Blocked nucleation sites decrease boiling heat transfer.
- Thermal conductivity effects are dominant than effect of nanoparticle layer on the boiling surface at low concentrations that is why HTC is higher at low concentrations.
- At high concentrations formation of extra thermal resistance decreases the HTC.
- During the nanofluids boiling, deposition of nanoparticle on heat transfer surface changes the microstructure and topography which are primary reasons of enhancing heat transfer.
- Deposition formed on heating surface changes the surface wettability, capillary wicking performance and surface roughness of boiling surface which increases heat transfer (BHT).
- Formation of vapour film around hot sphere during quenching process increases the boiling heat transfer.
- Active nucleation sites decrease with nanoparticle layers which significantly increases surface wettability (or less contact angle).

Acknowledgment

The authors greatly acknowledge the research facilities and financial support provided by University of Engineering and Technology Taxila, Punjab, Pakistan.

Nomenclature

d – thickness of thin film layer inside pore, [mm]
d_b – bubble departure diameter
f – frequency
fb – bubblele departure frequency
g – gravitational acceleration
h – enthalpy
h_{fg} – evaporation heat
h_{lv} – heat of vaporization
k – thermal conductivity of liquid, [$wm^{-2}k^{-1}$)
N_a' – number of active nucleate site density
P_r – Prandtl number
q'' – heat flux
q_{max} – heat flux at the onset of film boiling (hydrodynamic CHF/local dryout)
q_{max2} – Zuber's CHF prediction for infinite horizontal flat plates
R' – dimensionless radius
ΔT – temperature difference

Subscripts

b – bubble
bf – base fluid
nf – nanofluid
g – gas
l – liquid
v – vapor

Greek symbols

σ – surface tension
λ_m – modulation wavelength
μ – viscosity, [nsm^{-2}]
μ_f – fluid viscosity
ρ_l – density of liquid
ρ_v – density of vapour
Φ – nanoparticle volume fraction

Acronyms

ASNPS – alumina sponge-like nanoporous structure
BHF – burnout heat flux
CHF – critical heat flux
CNT – carbon nanofluid
DEG – diesel electric generator
EV – ethylene glycol
GO – graphene oxide
GON – graphide oxide nanosheets
HTC – heat transfer coefficient
IVR – in-vessel retention
LSMO – $La_{0.7}Sr_{0.3}MnO_3$
MFHP – miniature flat heat pipe
MNP – magnetic nanoparticles
MWNF – magnetite-water nanofluid

OA – oleic acid
RGO – reduced graphene oxide
SAM – self-assembled monolayer
SDS – sodium dodecyl sulfate
SDBS –sodium dodecyl benzene sulphonate

References

[1] Moita, A., *et al*., Influence of Surface Topography in the Boiling Mechanisms, *International Journal of Heat and Fluid Flow*, *52* (2015), Apr., pp. 50-63

[2] Hsu, C.-C., *et al*., Pool Boiling of Nanoparticle-Modified Surface with Interlaced Wettability, *Nanoscale Research Letters*, *7* (2012), 1, 259

[3] Lee, S., *et al*., Measuring Thermal Conductivity of Fluids Containing Oxide Nanoparticles, *Journal of Heat Transfer*, *121* (1999), 2, pp. 280-289

[4] Zhang, H., *et al*., Heat Transfer and Flow Features of Al_2O_3–Water Nanofluids Flowing through a Circular Microchannel–Experimental Results and Correlations, *Applied Thermal Engineering*, *61* (2013), 2, pp. 86-92

[5] Wan, Z., *et al*., Thermal Performance of a Miniature Loop Heat Pipe Using Water–Copper Nanofluid, *Applied Thermal Engineering*, *78* (2015), Mar., pp. 712-719

[6] Firouzfar, E., *et al*., Energy Saving in HVAC Systems Using Nanofluid, *Applied Thermal Engineering*, *31* (2011), 8, pp. 1543-1545

[7] Peyghambarzadeh, S., *et al*., Experimental Study of Overall Heat Transfer Coefficient in the Application of Dilute Nanofluids in the Car Radiator, *Applied Thermal Engineering*, *52* (2013), 1, pp. 8-16

[8] Delavari, V., Hashemabadi, S. H., CFD Simulation of Heat Transfer Enhancement of Al_2O_3/Water and Al_2O_3/Ethylene Glycol Nanofluids in a Car Radiator, *Applied Thermal Eng.*, *73* (2014), 1, pp. 380-390

[9] Rahman, M., *et al*., Effect of Solid Volume Fraction and Tilt Angle in a Quarter Circular Solar Thermal Collectors Filled with CNT–Water Nanofluid, *International Communications in Heat and Mass Transfer*, *57* (2014), Oct., pp. 79-90

[10] Mahian, O., *et al*., A Review of the Applications of Nanofluids in Solar Energy. *International Journal of Heat and Mass Transfer*, *57* (2013), 2, pp. 582-594

[11] Tseng, A. A., *et al*., Effects of Titania Nanoparticles on Heat Transfer Performance of Spray Cooling with Full Cone Nozzle, *Applied Thermal Engineering*, *62* (2014), 1, pp. 20-27

[12] Khaleduzzaman, S., *et al*., Energy and Exergy Analysis of Alumina-Water Nanofluid for an Electronic Liquid Cooling System, *International Communications in Heat and Mass Transfer*, *57* (2014), Oct., pp. 118-127

[13] Buongiorno, J., *et al*., Nanofluids for Enhanced Economics and Safety of Nuclear Reactors: an Evaluation of the Potential Features, Issues, and Research Gaps, *Nuclear Technology*, *162* (2008), 1, pp. 80-91

[14] Bang, I. C., Kim, J. H., Thermal-Fluid Characterizations of ZnO and SiC Nanofluids for Advanced Nuclear Power Plants, *Nuclear Technology*, 170 (2010), 1, pp. 16-27

[15] Buongiorno, J., *et al*., A Feasibility Assessment of the use of Nanofluids to Enhance the In-Vessel Retention Capability in Light-Water Reactors, *Nuclear Eng. and Design*, 239 (2009), 5, pp. 941-948

[16] Hong, T.-K., *et al*., Study of the Enhanced Thermal Conductivity of Fe Nanofluids, *Journal of Applied Physics*, *97* (2005), 6, 064311

[17] Das, S. K., *et al*., Pool Boiling Characteristics of Nano-Fluids, *International Journal of Heat and Mass Transfer*, *46* (2003), 5, pp. 851-862

[18] Taylor, R. A., Phelan,P. E., Pool Boiling of Nanofluids: Comprehensive Review of Existing Data and Limited New Data, *International Journal of Heat and Mass Transfer*, *52* (2009), 23, pp. 5339-5347

[19] You, S., *et al*., Effect of Nanoparticles on CHF of Water in Pool Boiling Heat Transfer, *Applied Physics Letters*, *83* (2003), 16, pp. 3374-3376

[20] Vassallo, P., *et al*., Pool Boiling Heat Transfer Experiments in Silica-Water Nano-Fluids, *International Journal of Heat and Mass Transfer*, *47* (2004), 2, pp. 407-411

[21] Bang, I. C., Chang, S. H., Boiling Heat Transfer Performance and Phenomena of Al_2O_3-Water Nano-Fluids from a Plain Surface in a Pool, *International Journal of Heat and Mass Transfer*, *48* (205), 12, pp 2407-2419

[22] Golubovic, M. N., *et al*., Nanofluids and CHF, Experimental and Analytical Study, *Applied Thermal Engineering*, 29 (2009), 7, pp. 1281-1288

[23] Kwark, S. M., *et al.*, Pool Boiling Characteristics of Low Concentration Nanofluids, *International Journal of Heat and Mass Transfer*, *53* (2010), 5, pp. 972-981

[24] Kim, S. J., *et al.,* Surface Wettability Change During Pool Boiling of Nanofluids and Its Effect on CHF. *International Journal of Heat and Mass Transfer*, *50* (2007), 19, pp. 4105-4116
[25] Coursey, J. S., Kim, J., Nanofluid Boiling: the Effect of Surface Wettability, *International Journal of Heat and Fluid Flow*, *29* (2008), 6, pp. 1577-1585
[26] Harish, G., *et al*., Effect of Surface Particle Interactions During Pool Boiling of Nanofluids, *International Journal of Thermal Sciences*, *50* (2010), 12, pp. 2318-2327
[27] Yang, X.-F., Liu, Z.-H., Application of Functionalized Nanofluid in Thermosyphon, *Nanoscale research letters, 6* (2011), 1, 494
[28] Yang, X., Liu, Z.-H., A Kind of Nanofluid Consisting of Surface-Functionalized Nanoparticles, *Nanoscale Research Letters, 5* (2010), 8, 1324
[29] Huang, C.-K., *et al*., Boiling Enhancement by TiO_2 Nanoparticle Deposition, *International Journal of Heat and Mass Transfer*, *54* (2011), 23, pp. 4895-4903
[30] Yang, Y. M., Maa, J. R., Boiling of Suspension of Solid Particles in Water, *International Journal of Heat and Mass Transfer*, *27* (1984), 1, pp. 145-147
[31] Kathiravan, R., *et al*., Characterization and Pool Boiling Heat Transfer Studies of Nanofluids, *Journal of Heat Transfer*, *131* (2009), 8, 081902
[32] Kim, H., *et al*., Effect of Nanoparticles on CHF Enhancement in Pool Boiling of Nano-Fluids, *International Journal of Heat and Mass Transfer*, *49* (2006), 25, pp. 5070-5074
[33] Liu, Z.-H., *et al*., Boiling Heat Transfer Characteristics of Nanofluids in a Flat Heat Pipe Evaporator with Micro-Grooved Heating Surface, *Int. Journal of Multiphase Flow*, *33* (2007), 12, pp. 1284-1295
[34] Truong, B., *et al*., Modification of Sandblasted Plate Heaters using Nanofluids to Enhance Pool Boiling CHF, *International Journal of Heat and Mass Transfer*, *53* (2010), 1, pp. 85-94
[35] Yang, X.-F., Liu, Z.-H., Pool Boiling Heat Transfer of Functionalized Nanofluid under Sub-Atmospheric Pressures, *International Journal of Thermal Sciences*, *50* (2011), 12, pp. 2402-2412
[36] Vazquez, D. M., Kumar, R., Surface Effects of Ribbon Heaters on CHF in Nanofluid Pool Boiling, *International Communications in Heat and Mass Transfer*, *41* (2013), Feb., pp. 1-9
[37] Sheikhbahai, M., *et al*.,, Experimental Investigation of Pool Boiling of Fe_3O_4/Ethylene Glycol–Water Nanofluid in Electric Field, *International Journal of Thermal Sciences*, *62* (2012), Dec., pp. 149-153
[38] Jung, J.-Y., *et al*., Stabilizer Effect on CHF and Boiling Heat Transfer Coefficient of Alumina/Water Nanofluids, *International Journal of Heat and Mass Transfer*, *55* (2012), 7, pp. 1941-1946
[39] Lee, J. H., *et al*., Experimental Study on the Pool Boiling CHF Enhancement using Magnetite-Water Nanofluids, *International Journal of Heat and Mass Transfer*, *55* (2012), 9, pp. 2656-2663
[40] Shahmoradi, Z., *et al*., Pool Boiling Characteristics of Nanofluid on Flat Plate Based on Heater Surface Analysis, *International Communications in Heat and Mass Transfer*, *47* (2013), Oct., pp. 113-120
[41] Park, S. D., *et al*., Effects of Thickness of Boiling-Induced Nanoparticle Deposition on the Saturation of CHF Enhancement, *International Journal of Heat and Mass Transfer*, *78* (2014), Nov., pp. 506-514
[42] Zhang, L., *et al*., An Experimental Investigation of Transient Pool Boiling of Aqueous Nanofluids with Graphene Oxide Nanosheets as Characterized by the Quenching Method, *International Journal of Heat and Mass Transfer*, *73* (2014), June, pp. 410-414
[43] Park, S. D., Bang, I. C., Experimental Study of a Universal CHF Enhancement Mechanism in Nanofluids Using Hydrodynamic Instability, *International Journal of Heat and Mass Transfer*, *70* (2014), Mar., pp. 844-850
[44] Lee, J. H., *et al*., The Effect of Pressure on the CHF in Water-Based Nanofluids Containing Al_2O_3 and Fe_3O_4 Nanoparticles, *International Journal of Heat and Mass Transfer*, *61* (2013), June, pp. 432-438
[45] Ahn, H. S., *et al*., Experimental Study of the Effect of a Reduced Graphene Oxide Coating on CHF Enhancement, *International Journal of Heat and Mass Transfer*, *60* (2013), May, pp. 763-771
[46] Milanova, D., Kumar, R., Role of Ions in Pool Boiling Heat Transfer of Pure and Silica Nanofluids. *Applied Physics Letters*, *87* (2005), 23, 233107
[47] Kim, J. M., *et al*., Effect of a Graphene Oxide Coating Layer on CHF Enhancement Under Pool Boiling, *International Journal of Heat and Mass Transfer*, *77* (2014), Oct., pp. 919-927
[48] Stutz, B., *et al.,* Influence of Nanoparticle Surface Coating on Pool Boiling, *Experimental Thermal and Fluid Science*, *35* (2011), 7, pp. 1239-1249
[49] Park, S. D., *et al.,* Effects of Nanofluids Containing Graphene/Graphene-Oxide Nanosheets on CHF. *Applied Physics Letters*, *97* (2010), 2, 023103
[50] You, S., *et al*., The Onset of Film Boiling on Small Cylinders: Local Dryout and Hydrodynamic CHF Mechanisms, *International Journal of Heat and Mass Transfer*, *37* (1994), 16, pp. 2561-2569

[51] Kim, H., *et al*., Effect of Nanoparticle Deposit Layer Properties on Pool Boiling CHF of Water from a thin Wire, *International Journal of Heat and Mass Transfer*, *69* (2014), Feb., pp. 164-172
[52] Sharma, V. I., *et al.,* Experimental Investigation of Transient CHF of Water-Based Zinc–Oxide Nanofluids, *International Journal of Heat and Mass Transfer*, *61* (2013), June, pp. 425-431
[53] Ahn, H. S., Kim, M. H., The Boiling Phenomenon of Alumina Nanofluid Near CHF, *International Journal of Heat and Mass Transfer*, *62* (2013), July, pp. 718-728
[54] Kathiravan, R., *et al.,* Preparation and Pool Boiling Characteristics of Copper Nanofluids over a Flat Plate Heater, *International Journal of Heat and Mass Transfer*, *53* (2010), 9, pp. 1673-1681
[55] Bolukbasi, A., Ciloglu, D., Pool Boiling Heat Transfer Characteristics of Vertical Cylinder Quenched by SiO_2–Water Nanofluids, *International Journal of Thermal Sciences*, *50* (2011), 6, pp. 1013-1021
[56] Ciloglu, D., Bolukbasi, A., The Quenching Behavior of Aqueous Nanofluids Around Rods with High Temperature, *Nuclear Engineering and Design*, *241* (2011), 7, pp. 2519-2527
[57] Sakashita, H., CHF and Near-Wall Boiling Behaviors in Pool Boiling of Water on a Heating Surface Coated with Nanoparticles, *Int. Journal of Heat and Mass Transfer*, *55* (2012), 23, pp. 7312-7320
[58] Jaikumar, A., Kandlikar, S. G., Enhanced Pool Boiling for Electronics Cooling using Porous Fin Tops on Open Microchannels with FC-87, *Applied Thermal Engineering*, *91* (2015), Dec., pp. 426-433
[59] Okawa, T., *et al*., Boiling Time Effect on CHF Enhancement in Pool Boiling of Nanofluids, *International Journal of Heat and Mass Transfer*, *55* (2012), 9, pp. 2719-2725
[60] Liu, Z.-H., Liao, L., Sorption and Agglutination Phenomenon of Nanofluids on a Plain Heating Surface During Pool Boiling, *International Journal of Heat and Mass Transfer*, *51* (2008), 9, pp. 2593-2602
[61] Liu, Z.-H., *et al*., Boiling Characteristics of Carbon Nanotube Suspensions Under Sub-Atmospheric Pressures, *International Journal of Thermal Sciences*, *49* (2010), 7, pp. 1156-1164
[62] Song, S. L., *et al*., CHF Enhancement of SiC Nanofluid in Pool Boiling Experiment, *Experimental Thermal and Fluid Science*, *52* (2014), Jan., pp. 12-18
[63] Mourgues, A., *et al.,* Boiling Behaviors and CHF on a Horizontal and Vertical Plate in Saturated Pool Boiling with and Without ZnO Nanofluid, *Int. J. of Heat and Mass Transfer*, *57* (2013), 2, pp. 595-607
[64] Mori, S., *et al*., Enhancement of the CHF in Saturated Pool Boiling of Water by Nanoparticle-Coating and a Honeycomb Porous Plate, *Int. Journal of Heat and Mass Transfer*, *80* (2015), Jan., pp. 1-6
[65] Jo, B., *et al.,* Wide Range Parametric Study for the Pool Boiling of Nano-Fluids with a Circular Plate Heater, *Journal of Visualization*, *12* (2009), 1, pp. 37-46
[66] Jung, J.-Y., *et al*., Effect of Ionic Additive on Pool Boiling CHF of Titania/Water Nanofluids, *Heat and Mass Transfer*, *49* (2013), 1, pp. 1-10
[67] Pham, Q., *et al.,* Enhancement of CHF Using Nano-Fluids for Invessel Retention–External Vessel Cooling. *Applied Thermal Engineering*, *35* (2012), Mar., pp. 157-165
[68] Hu, Y., *et al.,* Experimental and Numerical Investigation on Natural Convection Heat Transfer of TiO_2–Water Nanofluids in a Square Enclosure, *Journal of Heat Transfer*, *136* (2014), 2, 022502
[69] Raveshi, M. R., *et al.,* Experimental Investigation of Pool Boiling Heat Transfer Enhancement of Alumina-Water-Ethylene Glycol Nanofluids, *Exp. T. and Fluid Science*, *44* (2013), Jan., pp. 805-814
[70] Wen, D., Ding, Y., Experimental Investigation into the Pool Boiling Heat Transfer of Aqueous Based γ-Alumina Nanofluids, *Journal of Nanoparticle Research*, *7* (2005), 2, pp. 265-274
[71] Chopkar, M., *et al.,* Pool Boiling Heat Transfer Characteristics of ZrO_2–Water Nanofluids from a Flat Surface in a Pool, *Heat and Mass Transfer*, *44* (2008), 8, pp. 999-1004
[72] Tang, X., *et al*., Experimental Investigation of the Nucleate Pool Boiling Heat Transfer Characteristics of δ-Al_2O_3-R141b Nanofluids on a Horizontal Plate, *Experimental Thermal and Fluid Science*, *52* (2014), Jan., pp. 88-96
[73] Suriyawong, A., Wongwises, S., Nucleate Pool Boiling Heat Transfer Characteristics of TiO_2–Water Nanofluids at Very Low Concentrations, *Exp. Thermal and Fluid Science*, *34* (2010), 8, pp. 992-999
[74] Ahmed, O., Hamed, M., Experimental Investigation of the Effect of Particle Deposition on Pool Boiling of Nanofluids, *International Journal of Heat and Mass Transfer*, *55* (2012), 13, pp. 3423-3436
[75] White, S. B., *et al.,* Effects of Nanoparticle Layering on Nanofluid and Base Fluid Pool Boiling Heat Transfer from a Horizontal Surface Under Atmospheric Pressure, *Journal of Applied Physics*, *107* (2010), 11, 114302
[76] Akbari, E., *et al.,* Effect of Silver Nanoparticle Deposition in Re-Entrant Inclined Minichannel on Bubble Dynamics for Pool Boiling Enhancement, *Experimental Thermal and Fluid Science*, *82* (2017), Apr., pp. 390-401

[77] Phan, H. T., *et al.*, Surface Coating with Nanofluids: The Effects on Pool Boiling Heat Transfer, *Nanoscale and Microscale Thermophysical Engineering*, *14* (2010), 4, pp. 229-244
[78] Xu, Z., Zhao, C., Influences of Nanoparticles on Pool Boiling Heat Transfer in Porous Metals, *Applied Thermal Engineering*, *65* (2014), 1, pp. 34-41
[79] Jaikumar, A., *et al*., Pool Boiling Enhancement through Graphene and Graphene Oxide Coatings, *Heat Transfer Engineering*, *38* (2017), 14-15, pp. 1274-1284
[80] Ahn, H. S., *et al.*, Pool Boiling Experiments in Reduced Graphene Oxide Colloids, Part I–Boiling Characteristics, *International Journal of Heat and Mass Transfer*, 74 (2014), July, pp. 501-512
[81] Ganapathy, H., Sajith, V., Semi-Analytical Model for Pool Boiling of Nanofluids, *International Journal of Heat ond Mass Transfer*, *57* (2013), 1, pp. 32-47
[82] Shoghl, S. N., Experimental Investigation on Pool Boiling Heat Transfer of ZnO, and CuO Water-Based Nanofluids and Effect of Surfactant on Heat Transfer Coefficient, *International Communications in Heat and Mass Transfer*, *45* (2013), July, pp. 122-129
[83] Soltani, S., *et al*., Pool Boiling Heat Transfer Performance of Newtonian Nanofluids, *Heat and mass Transfer*, *45* (2009), 12, pp. 1555-1560
[84] Trisaksri, V., Wongwises, S., Nucleate Pool Boiling Heat Transfer of TiO_2–R141b Nanofluids, *International Journal of Heat and Mass Transfer*, *52* (2009), 5, pp. 1582-1588
[85] Kole, M., Dey, T., Thermal Performance of Screen Mesh Wick Heat Pipes Using Water-Based Copper Nanofluids, *Applied Thermal Engineering*, *50* (2013), 1, pp. 763-770
[86] Soltani, S., *et al*., Pool Boiling Heat Transfer of Non-Newtonian Nanofluids, *International Communications in Heat and Mass Transfer*, *37* (2010), 1, pp. 29-33
[87] Wen, D., Influence of Nanoparticles on Boiling Heat Transfer, *App. Ther. Eng.*, *41* (2012), Aug., pp. 2-9
[88] Wen, D., *et al.*, Boiling Heat Transfer of Nanofluids: The Effect of Heating Surface Modification, *International Journal of Thermal Sciences*, *50* (2011), 4, pp. 480-485
[89] Naphon, P., Thongjing, C., Pool Boiling Heat Transfer Characteristics of Refrigerant-Nanoparticle Mixtures, *International Communications in Heat and Mass Transfer*, *52* (2014), Mar., pp. 84-89
[90] Sarafraz, M., Hormozi, F., Pool Boiling Heat Transfer to Dilute Copper Oxide Aqueous Nanofluids, *International Journal of Thermal Sciences*, *90* (2015), Apr., pp. 224-237
[91] Sarafraz, M., Hormozi, F., Nucleate Pool Boiling Heat Transfer Characteristics of Dilute Al_2O_3–Ethyleneglycol Nanofluids, *Int. Commu. in Heat and Mass Transfer*, *58* (2014), Nov., pp. 96-104
[92] Lee, C. Y., *et al*., Influence of Heated Surfaces and Fluids on Pool Boiling Heat Transfer, *Experimental Thermal and Fluid Science*, *59* (2014), Nov., pp. 15-23
[93] Zhang, B. J., *et al*., Enhanced Heat Transfer Performance of Alumina Sponge-Like Nano-Porous Structures through Surface Wettability Control in Nucleate Pool Boiling, *International Journal of Heat and Mass Transfer*, *55* (2012), 25, pp. 7487-7498
[94] Sayahi, T., *et al*., A RBF Model for Predicting the Pool Boiling Behavior of Nanofluids over a Horizontal Rod Heater, *International Journal of Thermal Sciences*, *99* (2016), Jan., pp. 180-194
[95] Narayan, G. P., *et al*., Mechanism of Enhancement/Deterioration of Boiling Heat Transfer Using Stable Nanoparticle Suspensions over Vertical Tubes, *Journal of Applied Physics*, 102 (2007), 7, 074317
[96] Brinkman, H., The Viscosity of Concentrated Suspensions and Solutions, *The Journal of Chemical Physics*, 20 (1952), 4, pp. 571-571
[97] Namburu, P. K., *et al.*, Viscosity of Copper Oxide Nanoparticles Dispersed in Ethylene Glycol and Water Mixture, *Experimental Thermal and Fluid Science*, 32 (2007), 2, pp. 397-402
[98] Nguyen, C., *et al.*, Viscosity Data for Al_2O_3-Water Nanofluid-Hysteresis: Is Heat Transfer Enhancement Using Nanofluids Reliable?, *International Journal of Thermal Sciences*, 47 (2008), 2, pp. 103-111
[99] Khanafer, K., Vafai, K., A Critical Synthesis of Thermophysical Characteristics of Nanofluids, *International Journal of Heat and Mass Transfer*, 54 (2011), 19, pp. 4410-4428
[100] Kathiravan, R., *et al.*, Pool Boiling Characteristics of Multiwalled Carbon Nanotube (CNT) Based Nanofluids over a Flat Plate Heater, *Int. J. of Heat and Mass Transfer, 54* (2011), 5, pp. 1289-1296
[101] Vafaei, S., *et al.*, The Effect of Nanoparticles on the Liquid-Gas Surface Tension of Bi2Te3 Nanofluids, *Nanotechnology*, *20* (2009), 18, 185702
[102] Kumar, R., Milanova, D., Effect of Surface Tension on Nanotube Nanofluids, *Applied Physics Letters*, *94* (2009), 7, 073107
[103] Lotfi, H., Shafii, M., Boiling Heat Transfer on a High Temperature Silver Sphere in Nanofluid, *International Journal of Thermal Sciences*, *48* (2009), 12, pp. 2215-2220

[104] Li, J.-Q., *et al*. An Experimental Study of Boiling Heat Transfer During Quenching of Nanofluids with Carbon Nanotubes of Various Sizes, *Proceedings*, ASME 2016 Heat Transfer Summer Con. Collocated with the ASME 2016 Fluids Engineering Division Summer Meeting and the ASME 2016 14th Int. Con. on Nanochannels, Microchannels, and Minichannels, American Society of Mechanical Engineers, Washington DC, USA, 2016
[105] Hashemi, S. M. H., *et al*., Study of Heat Transfer Enhancement in a Nanofluid-Cooled Miniature Heat Sink, *International Communications in Heat and Mass Transfer*, *39* (2012), 6, pp. 877-884
[106] Sohel, M., *et al.*, Investigating the Heat Transfer Performance and Thermophysical Properties of Nanofluids in a Circular Micro-Channel, *Int. C. in Heat and Mass Transfer*, *42* (2013), Mar., pp. 75-81
[107] Salman, B., *et al.*, Characteristics of Heat Transfer and Fluid Flow in Microtube and Microchannel Using Conventional Fluids and Nanofluids: A Review, *Renewable and Sustainable Energy Reviews*, *28* (2013), Dec., pp. 848-880
[108] Fukada, Y., *et al*., The Effect of Fouling on Nucleate Pool Boiling of Small Wires, *Heat Transfer Asian Research*, *33* (2004), 5, pp. 316-329
[109] Betz, A. R., *et al.*, Do Surfaces with Mixed Hydrophilic and Hydrophobic Areas Enhance Pool Boiling? *Applied Physics Letters*, *97* (2010), 14, pp. 141909
[110] Gheitaghy, A. M., *et al*., Surface Structuring with Inclined Minichannels for Pool Boiling Improvement, *Applied Thermal Engineering*, *126* (2017), Nov., pp. 892-902
[111] Chu, K.-H., *et al*., Structured Surfaces for Enhanced Pool Boiling Heat Transfer, *Applied Physics Letters*, *100* (2012), 24, 241603
[112] Wang, C., Dhir, V., Effect of Surface Wettability on Active Nucleation Site Density During Pool Boiling of Water on a Vertical Surface, *Journal of Heat Transfer*, *115* (1993), 3, pp. 659-669
[113] Dehkordi, R. A., *et al*., Effects of Functionalized Single Walled Carbon Nanotubes on Thermal Performance of Antifreeze: An Experimental Study on Thermal Conductivity, *Applied Thermal Engineering*, *120* (2017), June, pp. 358-366
[114] Zuber, N., Hydrodynamic Aspects of Boiling Heat Transfer, Ph. D. thesis, Ramo-Wooldridge Corp., Los Angeles, Cal., USA; Univ. of California, Los Angeles, Cal., USA, 1959
[115] Zuber, N., Nucleate Boiling. The Region of Isolated Bubbles and the Similarity with Natural Convection, *International Journal of Heat and Mass Transfer*, *6* (1963), 1, pp. 53-78
[116] Rohsenow, W. M., *A Method of Correlating Heat Transfer Data for Surface Boiling of Liquids*, MIT Division of Industrial Cooporation, Cambridge, Mass., USA, 1951
[117] Zuber, N., On the Stability of Boiling Heat Transfer, *Trans. Am. Soc. Mech. Engrs*., *80* (1958)
[118] Kutateladze, S., On the transition to film boiling under natural convection, *Kotloturbostroenie*, *3* (1948), pp. 10-12
[119] Kandlikar, S. G., A Theoretical Model to Predict Pool Boiling CHF Incorporating Effects of Contact Angle and Orientation, *Journal of Heat Transfer*, 123 (2001), 6, pp. 1071-1079
[120] Zuber, N., The Hydrodynamic Crisis in Pool Boiling of Saturated and Subcooled Liquids. *Int. Developments in Heat Transfer, 27* (1961), pp. 230-236
[121] Lienhard, J., Dhir, V., On the Prediction of the Minimum Pool Boiling Heat Flux, *Journal of Heat Transfer*, *102* (1980), 3, pp. 457-460
[122] Haramura, Y., Katto, Y., A New Hydrodynamic Model of CHF, Applicable Widely to Both Pool and Forced Convection Boiling on Submerged Bodies in Saturated Liquids, *International Journal of Heat and Mass Transfer*, *26* (1983), 3, pp. 389-399
[123] Kandlikar, S. G., A Theoretical Model to Predict Pool Boiling CHF Incorporating Effects of Contact Angle and Orientation, *Transactions-American Society of Mechanical Engineers Journal of Heat Transfer*, *123* (2001), 6, pp.1071-1079
[124] Ferjančič, K., Golobič, I., Surface Effects on Pool Boiling CHF, *Experimental Thermal and Fluid Science*, *25* (2002), 7. pp. 565-571
[125] Ramilison, J., *et al*., Surface Factors Influencing Burnout on Flat Heaters, *Journal of Heat Transfer*, *114* (1992), 1, Series C, American Society of Mechanical Engineers, USA
[126] Nakayama, W., *et al.*, Dynamic Model of Enhanced Boiling Heat Transfer on Porous Surfaces – Part I: Experimental Investigation, *Journal of Heat Transfer*, *102* (1980), 3, pp. 445-450

Paper submitted: January 10, 2019
Paper revised: January 20, 2019
Paper accepted: February 10, 2019